R. & M. No. 3059
(18,001)
A.R.C. Technical Report

MINISTRY OF SUPPLY

AERONAUTICAL RESEARCH COUNCIL
REPORTS AND MEMORANDA

Calculation of Derivatives for a Cropped Delta Wing with an Oscillating Constant-Chord Flap in a Supersonic Air Stream

By

J. WATSON, B.Sc., B.A.,
of the Aerodynamics Division, N.P.L.

LONDON: HER MAJESTY'S STATIONERY OFFICE
1958
TWELVE SHILLINGS NET

Calculation of Derivatives for a Cropped Delta Wing with an Oscillating Constant-Chord Flap in a Supersonic Air Stream

By

J. WATSON, B.Sc., B.A.
of the Aerodynamics Division, N.P.L.

Reports and Memoranda No. 3059

November, 1955

Summary.—The lift, pitching moment and hinge moment are derived for a delta wing with a trailing-edge flap of constant chord when the wing is at zero incidence in a supersonic air stream and the flap oscillates harmonically with small amplitude and low frequency. It is assumed that the wing is sufficiently thin and the amplitude of oscillation sufficiently small to permit the use of linearised theory.

Expressions for the various control derivative coefficients are obtained for a particular delta wing of aspect ratio 1·8 and taper ratio 1/7. The investigation covers partial-span flaps; in each case there is a lower limit to the Mach numbers for which the theory applies, though from practical considerations this restriction is not serious. The derivatives are evaluated and tabulated for Mach numbers 1·1, 1·2, 1·4, 1·6, 2·0. The theory is shown to apply without appreciable error, provided that the frequency parameter based on mean chord does not exceed 0·4.

The calculated values of hinge-moment damping are compared with preliminary experimental values obtained at the National Physical Laboratory.

1. *Introduction.*—Complete sets of oscillatory derivatives for a delta wing of aspect ratio 1·8 and taper ratio 1/7 with control (Fig. 1) will be measured at the N.P.L. for Mach numbers up to $M = 1{\cdot}8$. This report considers theoretical derivatives when the flap alone is oscillating for comparison with the experimental data at supersonic speeds. The theory is formally applicable much nearer to $M = 1$ than is usually the case and the investigation offers the opportunity of assessing the usefulness of linearised theory near $M = 1$; in the full-span case, for example, the theory is applicable to a lower limit of $M = 1{\cdot}04$.

The aerodynamic loading is zero upstream of the hinge line of a thin plane delta wing of the plan-form shown in Fig. 1; the forces on the remainder of the wing were determined for low frequencies by Evvard's method (Ref. 1, 1950).

In section 3 the aerodynamic coefficients are calculated for the case of a full-span control and the extension to partial-span controls is given in section 4. The results of section 3 and section 4 are summarised at the end of section 4. The corresponding sets of derivatives for the delta wing with inboard or outboard controls are obtained in Section 5. The accuracy of the results and the ranges of Mach number for which they apply are discussed in section 6.

Published by permission of the Director, National Physical Laboratory.

2. *General Supersonic Theory.*—A method of calculating the forces acting on a wing is given by Evvard[1] (1950). The general equations of supersonic flow are linearised with respect to velocity and written in terms of an unsteady perturbation velocity potential. The linearisation leads to a linear partial differential equation satisfied by the perturbation velocity potential, which is simplified by certain transformations[2] (W. P. Jones, 1948) in the case of harmonic motion.

The square of the frequency is neglected. Thus the differential equation for general supersonic unsteady flow is transformed to the equation of steady flow at the particular Mach number $\sqrt{2}$.

2.1. *Governing Equation.*—The perturbation velocity potential, ϕ, satisfies

$$\frac{\partial^2\phi}{\partial t^2} + 2V\frac{\partial^2\phi}{\partial x\,\partial t} + V^2\frac{\partial^2\phi}{\partial x^2} = a^2\left(\frac{\partial^2\phi}{\partial x^2} + \frac{\partial^2\phi}{\partial y^2} + \frac{\partial^2\phi}{\partial z^2}\right), \quad .. \quad .. \quad .. \quad .. \quad (1)$$

where a = velocity of sound, V = velocity of air stream (Ref. 2, p. 1). With c_f as a length parameter, the transformations of x, y, z, t to the non-dimensional X, Y, Z, T

$$\left.\begin{aligned} x &= c_f X \cot\mu \\ y &= c_f Y \\ z &= c_f Z \\ t &= c_f T/V \end{aligned}\right\}, \quad .. \quad .. \quad .. \quad .. \quad .. \quad (2)$$

where $M = V/a$, $\cot\mu = \sqrt{(M^2 - 1)}$, are applied to equation (1).

In accordance with the assumption of simple harmonic motion ϕ is proportional to $e^{i\omega t} = e^{i\lambda T}$ and it is convenient to introduce a time-independent complex perturbation velocity potential Φ given by

$$\phi = \Phi \exp(i\lambda T - i\lambda X \sec^2\mu \cot\mu), \quad .. \quad .. \quad (3)$$

where $\lambda = \omega c_f/V$. Equation (3) combines with the transformations (2) to reduce (1) to

$$\frac{\partial^2\Phi}{\partial Y^2} + \frac{\partial^2\Phi}{\partial Z^2} - \frac{\partial^2\Phi}{\partial X^2} = k^2\Phi, \quad .. \quad .. \quad .. \quad .. \quad .. \quad .. \quad (4)$$

where $k = \lambda \sec\mu$. Since λ^2 is being neglected, (4) becomes

$$\frac{\partial^2\Phi}{\partial Y^2} + \frac{\partial^2\Phi}{\partial Z^2} - \frac{\partial^2\Phi}{\partial X^2} = 0, \quad .. \quad .. \quad .. \quad .. \quad .. \quad .. \quad .. \quad (5)$$

which is seen to correspond to steady motion at Mach number $\sqrt{2}$.

2.2. *Boundary Conditions over the Control.*—Under the assumptions of linearised theory, the control surface and the remaining triangular part of the wing may be treated as flat plates and the conditions over each may be referred to the plane $z = 0$, in which the triangular part is assumed to lie. Since the fluid flow is undisturbed until the hinge of the control is reached, ϕ is zero on and upstream of the wave front from the hinge. Further $(\partial\phi/\partial z)_{z=0}$ over the projection of the control on the plane $z = 0$ is determined by the motion of the control. These conditions are satisfied by Φ in the transformed ' X, Y, Z space '.

Let $\xi = \xi_0 e^{i\omega t}$ be the complex angle of control deflection (Fig. 2). Then $\zeta = x\xi = x\xi_0 e^{i\omega t}$ defines the downward displacement of points on the control surface. For tangential flow on the control

$$\begin{aligned} w_{z=0} &= \left(\frac{\partial\phi}{\partial z}\right)_{z=0} = \left(\frac{dz}{dt}\right)_{z=0} \\ &= -\left(\frac{\partial\zeta}{\partial t} + V\frac{\partial\zeta}{\partial x}\right)_{z=0} \\ &= -\xi_0 e^{i\omega t}(i\omega x + V) \\ &= -\xi_0 V e^{i\lambda T}(1 + i\lambda X \cot\mu). \end{aligned}$$

From equations (2) and (3):

$$\left(\frac{\partial \Phi}{\partial Z}\right)_{z=0} = c_f \left(\frac{\partial \Phi}{\partial z}\right)_{z=0}$$
$$= - c_f \xi_0 V(1 + i\lambda X \cot \mu) \exp (i\lambda X \sec^2 \mu \cot \mu)$$
$$= - \xi_0 c_f V(1 + i\lambda X \cot \mu)(1 + i\lambda X \sec^2 \mu \cot \mu) + 0(\lambda^2)$$
$$= - \xi_0 c_f V(1 + i\lambda K X) , \quad .. \quad .. \quad .. \quad .. \quad .. \quad .. \quad (6)$$

where $K = \cot \mu(1 + \sec^2 \mu)$.

The governing equation (5) and the boundary condition (6) in ' X, Y, Z space ' are independent of time and the solution Φ corresponds to a steady motion with $M = \sqrt{2}$. The forces on the delta wing are found from a knowledge of ϕ over the control surface.

3. *Full-span Control.*—The determination of ϕ over the control surface amounts to the determination of Φ on a rectangular region in the XY plane, bounded by the lines $X = 0$, l and $Y = \pm m$ (Fig. 3).

3.1. *Calculation of Velocity Potential.*—Due to the symmetry of the problem the region considered is the control surface on one half of the wing, $0 \leqslant X \leqslant l$, $0 \leqslant Y \leqslant m$, $Z = 0$, which is divided into region A, where the flow is two-dimensional, and region B, bounded by the wing tip (Fig. 3).

Let $\Phi(X, Y)$ denote the value of Φ at the point (X, Y) on the upper surface of the wing; then $\Phi = - \Phi(X, Y)$ on the lower surface. The solution $\Phi(X, Y)$ in each region (A and B) is found by Evvard's method in the case of steady flow at Mach number $\sqrt{2}$ (Ref. 1, equations (17) and (29)).

Region A.—In region A, $\Phi(X, Y)$ is given by a double integral over a region of the type S_1 (Fig. 3); from Ref. 1, equation (17)

$$\Phi(X, Y) = - \frac{1}{\pi\sqrt{2}} \iint_{S_1} \frac{\left(\frac{\partial \Phi}{\partial Z}\right)_{Z=0} dr_0 \, ds_0}{(r - r_0)^{1/2}(s - s_0)^{1/2}} , \quad .. \quad .. \quad .. \quad .. \quad .. \quad .. \quad (7)$$

where $r\sqrt{2} = (X - Y)$,

$s\sqrt{2} = (X + Y)$,

and S_1 is the region bounded by $X = 0$ and the forward ' Mach lines ' from the point (X, Y), that is, $r_0 + s_0 \geqslant 0$, $r_0 \leqslant r$, $s_0 \leqslant s$.

From equations (6) and (7)

$$\Phi(X, Y) = \frac{\xi_0 V c_f}{\pi\sqrt{2}} \iint_{S_1} \frac{\left[1 + i\lambda K \left(\frac{s_0 + r_0}{\sqrt{2}}\right)\right] dr_0 \, ds_0}{(r - r_0)^{1/2}(s - s_0)^{1/2}}$$
$$= \frac{\xi_0 V c_f}{\pi\sqrt{2}} \left[\int_{-s}^{r} \frac{dr_0}{(r - r_0)^{1/2}} \int_{-r_0}^{s} \frac{ds_0}{(s - s_0)^{1/2}} + \frac{i\lambda K}{\sqrt{2}} \int_{-s}^{r} \frac{dr_0}{(r - r_0)^{1/2}} \int_{-r_0}^{s} \frac{(s_0 + r_0) \, ds_0}{(s - s_0)^{1/2}}\right]$$
$$= \frac{\xi_0 V c_f}{\pi\sqrt{2}} \left[\int_{-s}^{r} \frac{2(s + r_0)^{1/2}}{(r - r_0)^{1/2}} dr_0 + \frac{i\lambda K}{\sqrt{2}} \int_{-s}^{r} \frac{4(s + r_0)^{3/2}}{3(r - r_0)^{1/2}} dr_0\right] \quad .. \quad .. \quad .. \quad (8)$$
$$= \frac{\xi_0 V c_f}{\pi\sqrt{2}} \left[\pi(r + s) + \frac{\pi i\lambda K}{2\sqrt{2}} (r + s)^2\right] .$$

When the expressions for r, s are substituted from equation (7), it follows that

$$\Phi(X, Y) = V\xi_0 c_f \left[X + \frac{i\lambda K}{2} X^2\right]. \quad .. \quad .. \quad .. \quad .. \quad .. \quad .. \quad .. \quad .. \quad (9)$$

This gives

$$\left(\frac{\partial \Phi}{\partial X}\right)_{Z=0} = V\xi_0 c_f[1 + i\lambda KX]. \quad .. \quad .. \quad .. \quad .. \quad .. \quad .. \quad .. \quad .. \quad (10)$$

Region B.—In region B, $\Phi(X, Y)$ is given by equation (7), where the double integral is taken over the region S_2 (Fig. 3), bounded by $X = Z = 0$ and the three Mach lines in the (X, Y) plane, that is, $r_0 + s_0 \geqslant 0$, $s - m\sqrt{2} \leqslant r_0 \leqslant r$, $s_0 \leqslant s$, where $s\sqrt{2} \geqslant m$ and r, s are given in equation (7). Thus $\Phi(X, Y)$ is given by equation (8) when the lower limit, $-s$, in the integrals is replaced by $s - m\sqrt{2}$. The integrations lead to

$$\begin{aligned}
\Phi(X, Y) = \frac{\xi_0 V c_f}{3\pi} \Bigg[& (3\sqrt{2})(s + r) \left\{ \sin^{-1} \left(\frac{(m\sqrt{2}) - s + r}{s + r} \right)^{1/2} \right. \\
& \left. + \sqrt{2}\, \frac{(s - \tfrac{1}{2}m\sqrt{2})^{1/2}\{(m\sqrt{2}) + r - s\}^{1/2}}{(s + r)} \right\} \\
& + i\lambda K \left\{ \frac{3}{2}(s + r)^2 \sin^{-1} \left(\frac{(m\sqrt{2}) - s + r}{s + r} \right)^{1/2} \right. \\
& \left. + \frac{1}{\sqrt{2}}(s - \tfrac{1}{2}m\sqrt{2})^{1/2}\{(m\sqrt{2}) + r - s\}^{1/2}(7s + 3r - 2m\sqrt{2}) \right\} \Bigg] \\
= \frac{V\xi_0 c_f}{3\pi} \Bigg[& 6X \sin^{-1} \left(\frac{m - Y}{X} \right)^{1/2} + 6(X + Y - m)^{1/2}(m - Y)^{1/2} \\
& + i\lambda K \left\{ 3X^2 \sin^{-1} \left(\frac{m - Y}{X} \right)^{1/2} \right. \\
& \left. + (5X + 2Y - 2m)(m - Y)^{1/2}(X + Y - m)^{1/2} \right\} \Bigg], \quad .. \quad .. \quad .. \quad .. \quad (11)
\end{aligned}$$

when X and Y are substituted from equation (7). From this expression it follows that

$$\begin{aligned}
\left(\frac{\partial \Phi}{\partial X}\right)_{Z=0} = \frac{2V\xi_0 c_f}{\pi} \Bigg[& \sin^{-1} \left(\frac{m - Y}{X} \right)^{1/2} \\
& + i\lambda K \left\{ X \sin^{-1} \left(\frac{m - Y}{X} \right)^{1/2} + (m - Y)^{1/2}(X + Y - m)^{1/2} \right\} \Bigg]. \quad .. \quad .. \quad (12)
\end{aligned}$$

3.2. *Calculation of Aerodynamic Coefficients.*—From equation (2*a*) of Ref. 1 the pressure on the upper surface of the control is

$$p_0 - \rho_0 \left(\frac{\partial \phi}{\partial t} + V \frac{\partial \phi}{\partial x} \right)_{z=0}.$$

Let P be the pressure difference across the control in the positive z direction. Then the lift per unit area is

$$P = 2\rho_0 \left(\frac{\partial \phi}{\partial t} + V\frac{\partial \phi}{\partial x}\right)_{z=0}$$

$$= \frac{2\rho_0 V}{c_f}\left(\frac{\partial \phi}{\partial T} + \tan\mu \frac{\partial \phi}{\partial X}\right)_{z=0}$$

$$= \frac{2\rho_0 V}{c_f}\exp\{i\lambda T - i\lambda X \sec^2\mu \cot\mu\}\left[i\lambda\Phi(X,Y) + \tan\mu\left\{\left(\frac{\partial \Phi}{\partial X}\right)_{Z=0}\right.\right.$$

$$\left.\left. - i\lambda\Phi(X,Y)\sec^2\mu \cot\mu\right\}\right]$$

$$= \frac{2\rho_0 V}{c_f \cot\mu}\exp\{i\lambda T - i\lambda X \sec^2\mu \cot\mu\}\left[\left(\frac{\partial \Phi}{\partial X}\right)_{Z=0} - i\lambda\Phi(X,Y)\tan\mu\right]$$

$$= \frac{2\rho_0 V\, e^{i\lambda T}}{c_f \cot\mu}\left[(1 - i\lambda X \sec^2\mu \cot\mu)\left(\frac{\partial \Phi}{\partial X}\right)_{Z=0} - i\lambda\Phi(X,Y)\tan\mu\right] + 0(\lambda^2)\,. \qquad (13)$$

In region A, P is obtained from equations (9), (10) and (13), where terms of order λ^2 are neglected. It is found that

$$P = \frac{4}{\pi}\rho_0 V^2 \xi_0 \tan\mu\, e^{i\lambda T}\, F\,, \qquad (14)$$

where

$$F = F_A = \tfrac{1}{2}\pi\{1 + i\lambda(\cot\mu - \tan\mu)X\}\,. \qquad (15)$$

Similarly, from equations (11), (12) and (13), in region B,

$$F = F_B = \sin^{-1}\left(\frac{m - Y}{X}\right)^{1/2}(1 - i\lambda X \sec^2\mu \cot\mu)$$

$$+ 2i\lambda \cot\mu\left\{X \sin^{-1}\left(\frac{m - Y}{X}\right)^{1/2} + (m - Y)^{1/2}(X + Y - m)^{1/2}\right\}. \qquad (16)$$

Hence the lift coefficient

$$C_L = \frac{L}{\frac{1}{2}\rho_0 V^2 S} = \frac{2\int_0^l \int_0^m P c_f\, dY\; c_f \cot\mu\, dX}{\frac{1}{2}\rho_0 V^2\; 2s\bar{c}}$$

$$= \frac{8}{\pi}\xi_0\, e^{i\lambda T}\frac{c_f^2}{s\bar{c}}\left[\iint_A F_A\, dX\, dY + \iint_B F_B\, dX\, dY\right], \qquad (17)$$

where, from equation (15)

$$\iint_A F_A\, dX\, dY = \int_0^l dX \int_0^{m-X} \tfrac{1}{2}\pi\{1 + i\lambda(\cot\mu - \tan\mu)X\}\, dY$$

$$= \tfrac{1}{2}\pi\int_0^l (m - X)\{1 + i\lambda(\cot\mu - \tan\mu)X\}\, dX$$

$$= \frac{1}{12}\pi l\left[3(2m - l) + i\lambda\left(\beta - \frac{1}{\beta}\right)l(3m - 2l)\right], \qquad (18)$$

where $\beta = \cot\mu = (M^2 - 1)^{1/2}$, $l = 1/\beta$, $m = s/c_f$ (Fig. 3), and from equation (16),

$$\iint_B F_B\,dX\,dY = \int_0^l dX \int_{m-X}^{m} \left[\sin^{-1}\left(\frac{m-Y}{X}\right)^{1/2}(1 - i\lambda X \sec^2\mu\ \cot\mu)\right.$$
$$\left. + 2i\lambda\cot\mu\left\{X\sin^{-1}\left(\frac{m-Y}{X}\right)^{1/2} + (m-Y)^{1/2}(X+Y-m)^{1/2}\right\}\right] dY$$
$$= \int_0^l \left[\frac{\pi X}{4}\{1 - i\lambda X\sec^2\mu\ \cot\mu\} + 2i\lambda\cot\mu\left\{\frac{\pi X^2}{4} + \frac{\pi X^2}{8}\right\}\right] dX$$
$$= \frac{\pi l^2}{24}\left[3 + 2i\lambda\left(2\beta - \frac{1}{\beta}\right)l\right]. \quad .. \quad .. \quad .. \quad .. \quad .. \quad .. \quad .. \quad (19)$$

Hence

$$C_L = \frac{\xi c_f^{\,2}}{s\bar{c}}\left[\left(-\frac{1}{\beta^2} + i\lambda\frac{2}{3\beta^4}\right) + \frac{2s}{c_f}\left\{\frac{2}{\beta} + i\lambda\left(\frac{1}{\beta} - \frac{1}{\beta^3}\right)\right\}\right]. \quad .. \quad .. \quad .. \quad (20)$$

Similarly, the pitching moment about the hinge is given by

$$-C_m = -\frac{\mathscr{M}}{\frac{1}{2}\rho_0 V^2 S\bar{c}}$$
$$= \frac{8}{\pi}\xi_0\,e^{i\lambda T}\frac{c_f^{\,3}}{s\bar{c}^2}\cot\mu\left[\iint_A XF_A\,dX\,dY + \iint_B XF_B\,dX\,dY\right]$$
$$= \xi\frac{c_f^{\,3}}{s\bar{c}^2}\left[\left(-\frac{2}{3\beta^2} + i\lambda\frac{1}{2\beta^4}\right) + \frac{2s}{c_f}\left\{\frac{1}{\beta} + \frac{2}{3}i\lambda\left(\frac{1}{\beta} - \frac{1}{\beta^3}\right)\right\}\right], \quad .. \quad .. \quad .. \quad (21)$$

and, since $H = \mathscr{M}$,

$$-C_H = -\frac{\mathscr{M}}{\frac{1}{2}\rho_0 V^2 S_f c_f} = -C_m\frac{\bar{c}^2}{c_f^{\,2}}$$
$$= \xi\frac{c_f}{s}\left[\left(-\frac{2}{3\beta^2} + i\lambda\frac{1}{2\beta^4}\right) + \frac{2s}{c_f}\left\{\frac{1}{\beta} + \frac{2}{3}i\lambda\left(\frac{1}{\beta} - \frac{1}{\beta^3}\right)\right\}\right]. \quad .. \quad .. \quad .. \quad (22)$$

The loading due to interference by the starboard tip ($F_B - F_A$), extends over the triangular region B (Fig. 3); a similar loading is due to the port tip effect. These may be superposed so long as the flow outboard of each tip is unaffected by the flow outboard of the other. Hence this analysis is valid provided that $c_f \leqslant 2\beta s$.

4. *Partial-span Controls.*—The most general control surface is shaded in Fig. 1. It will be shown that the loading can be expressed in terms of at most six fundamental perturbation velocity potentials, four of which are derived in section 4.1. The aerodynamic loading on an outboard control is considered in section 4.2 and section 4.3, where the condition is imposed that the Mach line from the leading-tip corner does not cross the inboard edge of the control, that is, η_1 must satisfy $\eta_1 \leqslant (1 - \varepsilon)$, where $\varepsilon = c_f/\beta s$. In section 4.4 the general control is treated subject to the Mach line from the leading-tip corner not crossing the outboard edge of the control, that is, $\eta_0 \leqslant (1 - \varepsilon)$. Up to this stage only four fundamental perturbation velocity potentials arise. The extension to the cases $(1 - \varepsilon) \leqslant \eta_1 \leqslant (1 - \frac{1}{2}\varepsilon)$ or $(1 - \varepsilon) \leqslant \eta_0 \leqslant (1 - \frac{1}{2}\varepsilon)$ in section 4.5 introduces a fifth potential. The sixth potential arises only when either $(1 - \frac{1}{2}\varepsilon) < \eta_1 \leqslant 1$ or $(1 - \frac{1}{2}\varepsilon) < \eta_0 \leqslant 1$; these cases are briefly considered in section 4.6, where a concluding table summarises the general equations for the aerodynamic coefficients.

By superposition and because of the symmetry of the flow about the centre-line it is sufficient to consider the deflection of one control only, the starboard control, say.

4.1. *Calculation of Fundamental Velocity Potentials.*—The simplest case of an outboard control, when the Mach lines from the leading corners of the control neither intersect on the plan-form nor cross the port control, is shown in the (X, Y) plane in Fig. 4. This corresponds to $\frac{1}{2}\varepsilon \leqslant \eta_1 \leqslant (1 - 2\varepsilon)$; to fix ideas, it is supposed that $\varepsilon < 2/5$. The outboard control covers the region $A + B + C$ in Fig. 4. Over the complete semi-span there are four regions, A, B, C, D, which correspond to different types of loading.

Regions A and B.—The complex velocity potential Φ as transformed by equation (3) is evaluated from the double integral (7), in which the area of integration in the plane $(r, s) \equiv \{(1/\sqrt{2})\,(X - Y),\ (1/\sqrt{2})\,(X + Y)\}$ depends on the region considered.

As shown in section 3.1, in the two-dimensional region A (Fig. 4), this leads to the expressions (9) and (10) for $\Phi(X,Y)$ and $(\partial\Phi/\partial X)_{z=0}$ and thence to equation (15) for the lift per unit area.

The region B for a partial-span control is equivalent to region B in section 3.1 (Fig. 3). It is convenient to translate the origin from 0 to 0_1 on the inboard edge of the control so that $Y_1 = Y - s\eta_1/c_f$ and at the wing tip

$$Y_1 = m_1 = \frac{s(1 - \eta_1)}{c_f} \quad \ldots\ldots\ldots\ldots\ldots\ldots\ldots\ldots \quad (23)$$

Then, in region B (Fig. 4), the expressions for $\Phi(X, Y)$ and $(\partial\Phi/\partial X)_{z=0}$ are given by equations (11) and (12) with $(m - Y)$ replaced by $(m_1 - Y_1)$. This leads to

$$F_B = \sin^{-1}\left(\frac{m_1 - Y_1}{X}\right)^{1/2}(1 - i\lambda X \sec^2\mu\ \cot\mu) + 2i\lambda \cot\mu \left\{X \sin^{-1}\left(\frac{m_1 - Y_1}{X}\right)^{1/2} + (m_1 - Y_1)^{1/2}\,(X + Y_1 - m_1)^{1/2}\right\}. \quad (24)$$

Region C.—In region C, $\Phi(X,Y_1)$ is evaluated from equation (7) with r, s, Y replaced by r_1, s_1, Y_1, where

$$\left.\begin{aligned} r_1\sqrt{2} &= (X - Y_1) \\ s_1\sqrt{2} &= (X + Y_1) \end{aligned}\right\} \quad \ldots\ldots\ldots\ldots\ldots\ldots\ldots\ldots \quad (25)$$

and the area of integration S_3 (Fig. 4) is given by $r_0 + s_0 \geqslant 0$, $s_0 \leqslant s_1$, $r_0 \leqslant r_1$, $s_0 - r_0 \geqslant 0$, where $0 \leqslant r_1 \leqslant s_1$. Thus

$$\begin{aligned}
\Phi(X, Y_1) &= \frac{\xi_0 V c_f}{\pi\sqrt{2}} \iint_{S_3} \frac{\left[1 + i\lambda K\left(\frac{s_0 + r_0}{\sqrt{2}}\right)\right]}{(r_1 - r_0)^{1/2}\,(s_1 - s_0)^{1/2}}\, dr_0\, ds_0 \\
&= \frac{\xi_0 V c_f}{\pi\sqrt{2}}\left[\int_{-s_1}^{0} \frac{dr_0}{(r_1 - r_0)^{1/2}} \int_{-r_0}^{s_1} \frac{ds_0}{(s_1 - s_0)^{1/2}} + \int_0^{r_1} \frac{dr_0}{(r_1 - r_0)^{1/2}} \int_{r_0}^{s_1} \frac{ds_0}{(s_1 - s_0)^{1/2}}\right. \\
&\quad + \frac{i\lambda K}{\sqrt{2}}\left\{\int_{-s_1}^{0} \frac{dr_0}{(r_1 - r_0)^{1/2}} \int_{-r_0}^{s_1} \frac{(s_0 + r_0)}{(s_1 - s_0)^{1/2}}\, ds_0\right. \\
&\quad \left.\left. + \int_0^{r_1} \frac{dr_0}{(r_1 - r_0)^{1/2}} \int_{r_0}^{s_1} \frac{(s_0 + r_0)\, ds_0}{(s_1 - s_0)^{1/2}}\right\}\right] \\
&= \frac{V\xi_0 c_f}{\pi\sqrt{2}}\left[\int_{-s_1}^{0} \frac{2(s_1 + r_0)^{1/2}}{(r_1 - r_0)^{1/2}}\, dr_0 + \int_0^{r_1} \frac{2(s_1 - r_0)^{1/2}}{(r_1 - r_0)^{1/2}}\, dr_0\right. \\
&\quad + \frac{i\lambda K}{\sqrt{2}}\left\{\int_{-s_1}^{0} \frac{4(s_1 + r_0)^{3/2}}{3(r_1 - r_0)^{1/2}}\, dr_0 + \int_0^{r_1} \frac{4(s_1 - r_0)^{1/2}\,(s_1 + 2r_0)}{3(r_1 - r_0)^{1/2}}\, dr_0\right\}\Big] \\
&= \frac{V\xi_0 c_f}{\pi\sqrt{2}}\left[2(s_1 + r_1)\left\{\frac{\pi}{2} - \sin^{-1}\left(\frac{r_1}{s_1 + r_1}\right)^{1/2}\right\}\right. \\
&\quad + 2(s_1 - r_1)\sinh^{-1}\left(\frac{r_1}{s_1 - r_1}\right)^{1/2} \\
&\quad + \frac{i\lambda K}{\sqrt{2}}\left\{(s_1 + r_1)^2\left(\frac{\pi}{2} - \sin^{-1}\left(\frac{r_1}{s_1 + r_1}\right)^{1/2}\right)\right. \\
&\quad \left.\left. + 2(s_1^2 - r_1^2)\sinh^{-1}\left(\frac{r_1}{s_1 - r_1}\right)^{1/2} - (s_1 - r_1)r_1^{1/2}s_1^{1/2}\right\}\Big].
\end{aligned}$$

Substitution for r_1, s_1 from (25) leads to

$$\Phi(X, Y_1) = \frac{V\xi_0 c_f}{\pi\sqrt{2}}\left[(2\sqrt{2})X\left\{\frac{\pi}{2} - \sin^{-1}\left(\frac{X-Y_1}{2X}\right)^{1/2}\right\} + (2\sqrt{2})Y_1 \sinh^{-1}\left(\frac{X-Y_1}{2Y_1}\right)^{1/2}\right.$$
$$+ \frac{i\lambda K}{\sqrt{2}}\left\{2X^2\left(\frac{\pi}{2} - \sin^{-1}\left(\frac{X-Y_1}{2X}\right)^{1/2}\right)\right.$$
$$\left.\left. + 4XY_1 \sinh^{-1}\left(\frac{X-Y_1}{2Y_1}\right)^{1/2} - Y_1(X^2 - Y_1^2)^{1/2}\right\}\right], \quad .. \quad .. \quad .. \quad (26)$$

and thence

$$\left(\frac{\partial\Phi}{\partial X}\right)_{Z=0} = \frac{2V\xi_0 c_f}{\pi}\left[\frac{\pi}{2} - \sin^{-1}\left(\frac{X-Y_1}{2X}\right)^{1/2}\right.$$
$$\left. + i\lambda K\left\{X\left(\frac{\pi}{2} - \sin^{-1}\left(\frac{X-Y_1}{2X}\right)^{1/2}\right) + Y_1 \sinh^{-1}\left(\frac{X-Y_1}{2Y_1}\right)^{1/2}\right\}\right]. \quad .. \quad (27)$$

The lift per unit area, P in region C is given by equations (13), (26) and (27). When terms of order λ^2 are neglected, P is given by equation (15), where

$$F = F_c = \frac{\pi}{2} - \sin^{-1}\left(\frac{X-Y_1}{2X}\right)^{1/2} + i\lambda\left(\beta - \frac{1}{\beta}\right)X\left(\frac{\pi}{2} - \sin^{-1}\left(\frac{X-Y_1}{2X}\right)^{1/2}\right)$$
$$+ 2i\lambda\beta Y_1 \sinh^{-1}\left(\frac{X-Y_1}{2Y_1}\right)^{1/2}. \quad .. \quad .. \quad .. \quad .. \quad .. \quad .. \quad (28)$$

Region D.—In region D, $\Phi(X,Y_1)$ is calculated similarly. Here the double integral is taken over the region S_4 (Fig. 4), given by $s_0 + r_0 \geqslant 0$, $s_0 - r_0 \geqslant 0$, $0 \leqslant s_0 \leqslant s_1 \leqslant r_1$. Thus

$$\Phi(X, Y_1) = \frac{\xi_0 V c_f}{\pi\sqrt{2}}\iint_{S_4}\frac{\left[1 + i\lambda K\left(\frac{s_0+r_0}{\sqrt{2}}\right)\right]}{(r_1 - r_0)^{1/2}(s_1 - s_0)^{1/2}}\,dr_0\,ds_0$$
$$= \frac{\xi_0 V c_f}{\pi\sqrt{2}}\left[\int_0^{s_1}\frac{ds_0}{(s_1-s_0)^{1/2}}\int_{-s_0}^{s_0}\frac{dr_0}{(r_1-r_0)^{1/2}} + \frac{i\lambda K}{\sqrt{2}}\int_0^{s_1}\frac{ds_0}{(s_1-s_0)^{1/2}}\int_{-s_0}^{s_0}\frac{(s_0+r_0)}{(r_1-r_0)^{1/2}}\,dr_0\right]$$
$$= \frac{\xi_0 V c_f}{\pi\sqrt{2}}\left[2\int_0^{s_1}\frac{\{(r_1+s_0)^{1/2} - (r_1-s_0)^{1/2}\}}{(s_1-s_0)^{1/2}}\,ds_0\right.$$
$$\left. + \frac{i\lambda K}{\sqrt{2}}\frac{4}{3}\int_0^{s_1}\frac{\{(r_1+s_0)^{3/2} - (r_1-s_0)^{1/2}(2s_0+r_1)\}}{(s_1-s_0)^{1/2}}\,ds_0\right]$$
$$= \frac{V\xi_0 c_f}{\pi\sqrt{2}}\left[2(r_1+s_1)\sin^{-1}\left(\frac{s_1}{r_1+s_1}\right)^{1/2} + 2(s_1-r_1)\sinh^{-1}\left(\frac{s_1}{r_1-s_1}\right)^{1/2}\right.$$
$$+ \frac{i\lambda K}{\sqrt{2}}\left\{(r_1+s_1)^2\sin^{-1}\left(\frac{s_1}{r_1+s_1}\right)^{1/2} + 2(s_1^2 - r_1^2)\sinh^{-1}\left(\frac{s_1}{r_1-s_1}\right)^{1/2}\right.$$
$$\left.\left. - (s_1 - r_1)r_1^{1/2}s_1^{1/2}\right\}\right].$$

Substitution for r_1, s_1 from (25) leads to

$$\Phi(X, Y_1) = \frac{V\xi_0 c_f}{\pi\sqrt{2}}\left[(2\sqrt{2})X\sin^{-1}\left(\frac{X+Y_1}{2X}\right)^{1/2} + (2\sqrt{2})Y_1\sinh^{-1}\left\{-\frac{X+Y_1}{2Y_1}\right\}^{1/2}\right.$$
$$+\frac{i\lambda K}{\sqrt{2}}\left\{2X^2\sin^{-1}\left(\frac{X+Y_1}{2X}\right)^{1/2}\right.$$
$$\left.\left.+4XY_1\sinh^{-1}\left(-\frac{X+Y_1}{2Y_1}\right)^{1/2} - Y_1(X^2-Y_1^2)^{1/2}\right\}\right], \quad .. \quad .. \quad .. \quad (29)$$

from which

$$\left(\frac{\partial\Phi}{\partial X}\right)_{Z=0} = \frac{2V\xi_0 c_f}{\pi}\left[\sin^{-1}\left(\frac{X+Y_1}{2X}\right)^{1/2} + i\lambda K\left\{X\sin^{-1}\left(\frac{X+Y_1}{2X}\right)^{1/2}\right.\right.$$
$$\left.\left.+Y_1\sinh^{-1}\left(-\frac{X+Y_1}{2Y_1}\right)^{1/2}\right\}\right]. \quad .. \quad .. \quad .. \quad .. \quad .. \quad .. \quad (30)$$

Equations (29) and (30) are treated in the same way as equations (26) and (27), so that the lift per unit area is given by equation (15), where, in region D,

$$F = F_D = \sin^{-1}\left(\frac{X+Y_1}{2X}\right)^{1/2} + i\lambda\left(\beta - \frac{1}{\beta}\right)X\sin^{-1}\left(\frac{X+Y_1}{2X}\right)^{1/2}$$
$$+2i\lambda\beta Y_1\sinh^{-1}\left(-\frac{X+Y_1}{2Y_1}\right)^{1/2}. \quad .. \quad .. \quad .. \quad .. \quad .. \quad .. \quad (31)$$

Two other fundamental velocity potentials arise in Section 4.5 and section 4.6; the corresponding regions of integration are shown shaded in Figs. 5 and 6. Expressions for these and for the corresponding loading functions, F_E and F_F, are derived in Appendices A and B.

4.2. *Outboard Control* $\frac{1}{2}\varepsilon \leqslant \eta_1 \leqslant (1-2\varepsilon)$.—Consider firstly the simple case of flow as represented in Fig. 4. Here the lift coefficient is given by (17) with additional integrals over C and D. The region A in Fig. 4 is seen to correspond to twice that in Fig. 3, with $2m$ replaced by m_1. When equation (18) is adapted in this way

$$\iint_A F_A\,dX\,dY_1 = \frac{1}{12}\pi l\left[6(m_1-l) + i\lambda\left(\beta - \frac{1}{\beta}\right)l(3m_1-4l)\right]. \quad .. \quad .. \quad .. \quad .. \quad (32)$$

Equation (24) is integrated to give equation (19) and m_1 and Y_1 in place of m and Y. Hence

$$\iint_B F_B\,dX\,dY_1 = \frac{1}{24}\pi l^2\left[3 + 2i\lambda\left(2\beta - \frac{1}{\beta}\right)l\right]. \quad .. \quad .. \quad .. \quad .. \quad .. \quad .. \quad (33)$$

From equation (28) and Fig. 4:

$$\iint_C F_C\,dX\,dY_1 = \int_0^l dX\int_0^X F_C\,dX\,dY_1$$
$$= \int_0^l dX\int_0^X\left[\frac{\pi}{2} - \sin^{-1}\left(\frac{X-Y_1}{2X}\right)^{1/2} + i\lambda\left(\beta - \frac{1}{\beta}\right)X\left\{\frac{\pi}{2} - \sin^{-1}\left(\frac{X-Y_1}{2X}\right)^{1/2}\right\}\right.$$
$$\left.+2i\lambda\beta Y_1\sinh^{-1}\left(\frac{X-Y_1}{2Y_1}\right)^{1/2}\right]dY_1$$
$$= \int_0^l\left[\frac{\pi}{2}X - \frac{X}{2} + i\lambda\left(\beta - \frac{1}{\beta}\right)X\left\{\frac{\pi}{2}X - \frac{X}{2}\right\} + 2i\lambda\beta\frac{X^2}{4}\right]dX$$
$$= \frac{l^2}{12}\left[(\pi-1)\left\{3 + 2i\lambda l\left(\beta - \frac{1}{\beta}\right)\right\} + 2i\lambda\beta l\right]. \quad .. \quad .. \quad .. \quad .. \quad (34)$$

From equation (31) similarly:

$$\iint_D F_D\,dX\,dY_1 = \int_0^l dX \int_{-X}^{0} F_D\,dY_1 = \int_0^l dX \int_0^X F_D\,d|Y_1|$$
$$= \int_0^l dX \int_0^X \left[\sin^{-1}\left(\frac{X-|Y_1|}{2X}\right)^{1/2} + i\lambda\left(\beta - \frac{1}{\beta}\right) X \sin^{-1}\left(\frac{X-|Y_1|}{2X}\right)^{1/2}\right.$$
$$\left. - 2i\lambda\beta\,|Y_1|\,\sinh^{-1}\left(\frac{X-|Y_1|}{2|Y_1|}\right)^{1/2}\right] d|Y_1|$$
$$= \int_0^l \left[\frac{X}{2} + i\lambda\left(\beta - \frac{1}{\beta}\right)\frac{X^2}{2} - 2i\lambda\beta\,\frac{X^2}{4}\right] dX$$
$$= \frac{l^2}{12}\left[3 - \frac{2i\lambda l}{\beta}\right]. \quad .. \quad .. \quad .. \quad .. \quad .. \quad .. \quad .. \quad .. \quad (35)$$

From equation (17) the lift coefficient for the pair of outboard controls is

$$C_L = \frac{8}{\pi}\,\xi\,\frac{c_f^{\,2}}{s\bar{c}} \iint F\,dX\,dY_1\,,$$

where, by summation of equations (32), (33), (34) and (35),

$$\iint F\,dX\,dY_1 = \frac{\pi l}{8}(4m_1 - l) + i\lambda\,\frac{\pi l^2}{12}\left\{3m_1\left(\beta - \frac{1}{\beta}\right) + \frac{l}{\beta}\right\}.$$

Since in Fig. 4, $l = 1/\beta$ and $m_1 = (s/c_f)\,(1 - \eta_1)$, it follows that

$$C_L = \frac{\xi c_f^{\,2}}{s\bar{c}}\left[\left(-\frac{1}{\beta^2} + i\lambda\,\frac{2}{3\beta^4}\right) + 2\tau_1\left\{\frac{2}{\beta^2} + i\lambda\left(\frac{1}{\beta^2} - \frac{1}{\beta^4}\right)\right\}\right], \quad .. \quad .. \quad .. \quad (36)$$

where

$$\tau_1 = \beta s(1 - \eta_1)/c_f\,. \quad .. \quad .. \quad .. \quad .. \quad .. \quad .. \quad .. \quad .. \quad (37)$$

This is identical to (20) with $2s$ replaced by $2s(1 - \eta_1)$, the total span of control.

Similarly, the pitching moment about the hinge is given by

$$-C_m = \frac{8}{\pi}\,\xi\,\frac{c_f^{\,3}}{s\bar{c}^2}\,\beta\left[\iint_A XF_A\,dX\,dY_1 + \iint_B XF_B\,dX\,dY_1\right.$$
$$\left. + \iint_C XF_C\,dX\,dY_1 + \iint_D XF_D\,dX\,dY_1\right],$$

where

$$\iint_A XF_A\,dX\,dY_1 = \frac{\pi}{8}\left[-\frac{8}{3\beta^3} - 2i\lambda\left(\frac{1}{\beta^3} - \frac{1}{\beta^5}\right) + \frac{2s}{c_f}(1 - \eta_1)\left\{\frac{1}{\beta^2} + i\lambda\,\frac{2}{3}\left(\frac{1}{\beta^2} - \frac{1}{\beta^4}\right)\right\}\right], \quad .. \quad (38)$$

$$\iint_B XF_B\,dX\,dY_1 = \frac{\pi}{8}\left[\frac{2}{3\beta^3} + i\lambda\tfrac{1}{2}\left(\frac{2}{\beta^3} - \frac{1}{\beta^5}\right)\right], \quad .. \quad .. \quad .. \quad .. \quad .. \quad .. \quad (39)$$

$$\iint_C XF_C\,dX\,dY_1 = \frac{\pi}{8}\left[\frac{4}{3\beta^3} + i\lambda\left(\frac{1}{\beta^3} - \frac{1}{\beta^5}\right)\right] - \frac{1}{6\beta^3} + \frac{i\lambda}{8\beta^5}, \quad .. \quad .. \quad .. \quad .. \quad .. \quad (40)$$

and

$$\iint_D XF_D\,dX\,dY_1 = \frac{1}{6\beta^3} - \frac{i\lambda}{8\beta^5}. \quad .. \quad .. \quad .. \quad .. \quad .. \quad .. \quad .. \quad .. \quad (41)$$

Hence

$$-C_m = \frac{\xi c_f^{\,3}}{s\bar{c}^2}\left[\left(-\frac{2}{3\beta^2} + i\lambda\,\frac{1}{2\beta^4}\right) + 2\tau_1\left\{\frac{1}{\beta^2} + i\lambda\tfrac{2}{3}\left(\frac{1}{\beta^2} - \frac{1}{\beta^4}\right)\right\}\right], \quad .. \quad .. \quad (42)$$

which is consistent with (21).

Similarly, from equations (38), (39) and (40), the hinge moment is given by (Fig. 4):

$$-C_H = \frac{8}{\pi}\xi\frac{c_f}{s(1-\eta_1)}\beta\left[\iint_A XF_A\,dX\,dY_1 + \iint_B XF_B\,dX\,dY_1 + \iint_C XF_C\,dX\,dY_1\right]$$
$$= \frac{\xi c_f}{s(1-\eta_1)}\left[\left(1+\frac{2}{\pi}\right)\left(-\frac{2}{3\beta^2}+i\lambda\frac{1}{2\beta^4}\right)+2\tau_1\left\{\frac{1}{\beta^2}+i\lambda\tfrac{2}{3}\left(\frac{1}{\beta^2}-\frac{1}{\beta^4}\right)\right\}\right]. \qquad (43)$$

4.3. *Outboard Control* $\eta_1 \leqslant (1-\varepsilon)$.—The aerodynamic coefficients C_L, C_m and C_H in equations (36), (42) and (43) apply when $\frac{1}{2}\varepsilon \leqslant \eta_1 \leqslant (1-2\varepsilon)$, where $\varepsilon = c_f/\beta s$; corrections to these expressions may be necessary when η_1 is outside this range.

The range $(1-2\varepsilon) < \eta_1 \leqslant (1-\varepsilon)$ is considered first (Fig. 7). Here the Mach lines from 0_1 and from the leading-tip corner intersect on the control. $F = F_A, F_B, F_C, F_D$ in regions R_1, R_2, R_3, R_4. So if $F_B = F_A + F_B'$, $F_C = F_A + F_C'$, then F_B' and F_C' represent the loading due to interference by the tip and the inboard edge of the control respectively. Hence, in region R_5, where the flow is influenced by both effects, it is clear that

$$F = F_A + F_B' + F_C' = F_B + F_C - F_A \ldots \qquad (44)$$

Further, the load distribution in Fig. 7 is composed of the loads F_D in R_4, F_A in $R_1 + R_2 + R_3 + R_5$, F_B' in $R_2 + R_5$ and F_C' in $R_3 + R_5$, while the distribution in Fig. 4 is composed of F_D in D, F_A in $A + B + C$, F_B' in B and F_C' in C. The integrals $\iint F$, $\iint XF$ in the two cases are therefore formally equivalent, so that equations (36), (42) and (43) are valid for $(1-2\varepsilon) < \eta_1 \leqslant (1-\varepsilon)$.

The formulae for C_L and C_m are easily seen to hold for $0 \leqslant \eta_1 < \frac{1}{2}\varepsilon$. However, there will be an increment, ΔC_H in the hinge-moment coefficient when the deflection of the control induces a loading on the port control.

This increment is given by

$$-\Delta C_H = \frac{8}{\pi}\frac{\xi c_f}{s(1-\eta_1)}\beta\iint_G XF_D\,dX\,dY_1, \qquad (45)$$

where, from Fig. 8 and equation (31),

$$\iint_G XF_D\,dX\,dY_1 = \int_{2(m-m_1)}^{l} dX\int_{-X}^{-2(m-m_1)} XF_D\,dY_1$$
$$= \int_{2(m-m_1)}^{l} X\left\{\tfrac{1}{2}(X^2-4(m-m_1)^2)^{1/2} - 2(m-m_1)\sin^{-1}\left(\frac{X-2m+2m_1}{2X}\right)^{1/2}\right\}dX$$
$$+ i\lambda\left(\beta-\frac{1}{\beta}\right)\int_{2(m-m_1)}^{l} X^2\left\{\tfrac{1}{2}(X^2-4(m-m_1)^2)^{1/2}\right.$$
$$\left. - 2(m-m_1)\sin^{-1}\left(\frac{X-2m+2m_1}{2X}\right)^{1/2}\right\}dX$$
$$- 2i\lambda\beta\int_{2(m-m_1)}^{l} X\left\{\tfrac{1}{4}X(X^2-4(m-m_1)^2)^{1/2}\right.$$
$$\left. - 2(m-m_1)^2\sinh^{-1}\left(\frac{X-2m+2m_1}{4(m-m_1)}\right)^{1/2}\right\}dX$$
$$= \frac{1}{12\beta^3}\{(2+\tau^2)(1-\tau^2)^{1/2} - 3\tau\cos^{-1}\tau\}$$
$$+ \frac{i\lambda}{24\beta^3}\left[-\tau^2(1-\tau^2)^{1/2} - 4\tau\cos^{-1}\tau + \tau^2(6-\tau^2)\cosh^{-1}\left(\frac{1}{\tau}\right)\right]$$
$$- \frac{i\lambda}{48\beta^5}\left[(6+\tau^2)(1-\tau^2)^{1/2} - 8\tau\cos^{-1}\tau + \tau^4\cosh^{-1}\left(\frac{1}{\tau}\right)\right], \ldots \qquad (46)$$

when l is replaced by $1/\beta$ and $\{2(m-m_1)\}/l = 2\beta s\eta_1/c_f$ is denoted by τ. This equation holds provided that $0 \leqslant 2(m-m_1) \leqslant l$, i.e., $0 \leqslant \tau \leqslant 1$.

It is convenient to introduce a function

$$f(\tau, \beta) = \frac{8\beta}{\pi}\iint_G XF_D\, dX\, dY_1 \qquad (0 \leqslant \tau \leqslant 1) \quad .. \quad .. \quad .. \quad .. \quad .. \quad (47)$$

$$= \frac{8\beta}{\pi} \text{ (Right-hand side of equation (46)),}$$

which vanishes when $\tau = 1$ and is identically zero for $\tau \geqslant 1$.

In the special case $\tau = 0$

$$f(0, \beta) = -\frac{2}{\pi}\left(-\frac{2}{3\beta^2} + i\lambda\frac{1}{2\beta^4}\right). \quad .. \quad .. \quad .. \quad .. \quad .. \quad .. \quad .. \quad (48)$$

When equations (43) and (45) are added together, the hinge moment for an outboard control such that $0 \leqslant \eta_1 \leqslant (1 - \varepsilon)$ is given by

$$-C_H = \frac{\xi c_f}{s(1-\eta_1)}\left[2\tau_1\left\{\frac{1}{\beta^2} + \tfrac{2}{3}i\lambda\left(\frac{1}{\beta^2} - \frac{1}{\beta^4}\right)\right\} - \left(1 + \frac{\pi}{2}\right)f(0, \beta) + f(\tau, \beta)\right], \qquad (49)$$

where $\tau = 2\eta_1/\varepsilon$ and $f(\tau, \beta)$ is defined in equation (47). This is seen to be identical to equation (43) when $\frac{1}{2}\varepsilon \leqslant \eta_1 \leqslant (1 - \varepsilon)$, since $f(\tau,\beta) = 0$ and $f(0, \beta)$ is given by (48).

For the same range the lift and pitching moment are given by equations (36) and (42). It is easily verified that as $\eta_1 \to 0$, equations (36), (42) and (49) reduce to the respective equations (20), (21) and (22) for a full-span control.

4.4. *General Control* ($\eta_0 \leqslant 1 - \varepsilon$).—The restriction is imposed that the Mach line from the leading-tip corner does not cut the outboard edge of the control, that is, $0 \leqslant \eta_1 \leqslant \eta_0 \leqslant (1 - \varepsilon)$, so that the flow will be symmetrical about $y = \frac{1}{2}s(\eta_0 + \eta_1)$. Such a control may be regarded as the difference between two outboard controls whose inboard edges are at $y = s\eta_0$ and $y = s\eta_1$. By superposition, it follows from equations (36) and (42) that

$$C_L = \xi 2\frac{c_f^2}{s\bar{c}}(\tau_1 - \tau_0)\left[\frac{2}{\beta^2} + i\lambda\left(\frac{1}{\beta^2} - \frac{1}{\beta^4}\right)\right] \quad .. \quad .. \quad .. \quad .. \quad .. \quad (50)$$

and

$$-C_m = \xi\frac{c_f^3}{s\bar{c}^2}\chi, \quad .. \quad .. \quad .. \quad .. \quad .. \quad .. \quad .. \quad .. \quad .. \quad (51)$$

for $0 \leqslant \eta_1 \leqslant \eta_0 \leqslant (1 - \varepsilon)$, where

$$\tau_0 = \frac{\beta s(1 - \eta_0)}{c_f} \quad .. \quad .. \quad .. \quad .. \quad .. \quad .. \quad .. \quad .. \quad (52)$$

and

$$\chi = 2(\tau_1 - \tau_0)\left[\frac{1}{\beta^2} + i\lambda\tfrac{2}{3}\left(\frac{1}{\beta^2} - \frac{1}{\beta^4}\right)\right]. \quad .. \quad .. \quad .. \quad .. \quad .. \quad (53)$$

It remains to obtain the expression for hinge-moment coefficient for $0 \leqslant \eta_1 \leqslant \eta_0 \leqslant (1 - \varepsilon)$, which is best derived by removing part of the pitching moment in equation (51).

Consider first the simplest case, when the flows over the outboard controls with inboard edges at $Y = s\eta_1/c_f$, $s\eta_0/c_f$ are of the type shown in Fig. 4. The difference is shown in Fig. 9 when the Mach line from 0_1 does not cut the outboard edge of the control, that is, when $\eta_0 - \eta_1 \geqslant \varepsilon$. This configuration applies provided that $\eta_0 \leqslant (1 - \varepsilon)$.

Since the flow is symmetrical about the line $Y = s(\eta_0 + \eta_1)/2c_f$, it follows that

$$\frac{1}{(\eta_0 - \eta_1)} \frac{\bar{c}^2}{c_f^2}(-C_m) - (-C_H) = \frac{2\xi c_f}{s(\eta_0 - \eta_1)} \frac{8\beta}{\pi} \iint XF_D \, dX \, dY_1 , \quad .. \quad .. \quad .. \quad (54)$$

where $-C_m$ is given by equation (51) and the integral is taken over the triangle with vertices $(X, Y_1) = (0, 0), (l, 0), (l, -l)$. Hence for $\frac{1}{2}\varepsilon \leqslant \eta_1 \leqslant \eta_0 \leqslant (1 - \varepsilon)$, $\eta_0 - \eta_1 \geqslant \varepsilon$,

$$-C_H = \frac{\xi c_f}{s(\eta_0 - \eta_1)} \{\chi - 2f(0, \beta)\} , \quad .. \quad .. \quad .. \quad .. \quad .. \quad .. \quad (55)$$

where $f(0, \beta)$ is given in equation (48).

The extension to $0 \leqslant \eta_1 < \frac{1}{2}\varepsilon$ corresponds exactly to the outboard control case considered in Fig. 8. The loading induced on a triangular area of the port control gives rise to the same increase in hinge moment as equation (45). This amounts to increasing χ in equation (55) by $f(2\eta_1/\varepsilon, \beta)$ in equation (47), so that

$$-C_H = \frac{\xi c_f}{s(\eta_0 - \eta_1)} \{\chi - 2f(0, \beta) + f(2\eta_1/\varepsilon, \beta)\} \quad .. \quad .. \quad .. \quad .. \quad (56)$$

for $0 \leqslant \eta_1 < \frac{1}{2}\varepsilon < \eta_0 \leqslant (1 - \varepsilon)$, $\eta_0 - \eta_1 \geqslant \varepsilon$.

Since $f(\tau, \beta) = 0$ for $\tau \geqslant 1$, then (56) reduces to (55) for $\eta_1 \geqslant \frac{1}{2}\varepsilon$ so that equation (56) holds for $0 \leqslant \eta_1 \leqslant \eta_0 \leqslant (1 - \varepsilon)$, $\eta_0 - \eta_1 \geqslant \varepsilon$.

Consider next the difference between two flows of the type shown in Fig. 4 when $\eta_0 - \eta_1 < \varepsilon$. The resulting flow is shown in Fig. 10, where one Mach line from 0_0 cuts the inboard edge of the control but the other does not cut the wing tip $\{\eta_0 \leqslant (1 - \varepsilon)\}$. Fig. 10 shows four distinct positions of the port control:

abb′ a′	—	$2\eta_1 \geqslant \varepsilon$
bcc′ b′	$2\eta_1 \leqslant \varepsilon$	$\eta_0 + \eta_1 \geqslant \varepsilon$
cdd′ c′	$\eta_0 + \eta_1 \leqslant \varepsilon$	$2\eta_0 \geqslant \varepsilon$
dee′ d′	$2\eta_0 \leqslant \varepsilon$	—

It will be remembered that the region with loading F_D in Fig. 9 leads to a term $-f(0, \beta)$ in equation (54). An identical term comes from the corresponding region outboard of the control. It is easily seen from Fig. 10 that both terms need to be replaced by

$$-\{f(0, \beta) - f[\{(\eta_0 - \eta_1)/\varepsilon\}, \beta]\}.$$

Thus, when the port control is in the region abb′ a′ and there is no interference between the controls,

$$-C_H = \frac{\xi c_f}{s(\eta_0 - \eta_1)} \left[\chi - 2f(0, \beta) + 2f\left(\frac{\eta_0 - \eta_1}{\varepsilon}, \beta\right)\right] \ldots \quad .. \quad .. \quad .. \quad (57)$$

When the Mach line from 0_1 cuts the port control but that from 0_0 does not, χ must be increased by $f(2\eta_1/\varepsilon, \beta)$ as in Fig. 8. Thus, when the port control is in the region bcc′ b′,

$$-C_H = \frac{\xi c_f}{s(\eta_0 - \eta_1)} \left[\chi - 2f(0, \beta) + 2f\left(\frac{\eta_0 - \eta_1}{\varepsilon}, \beta\right) + f\left(\frac{2\eta_1}{\varepsilon}, \beta\right)\right]. \quad .. \quad (58)$$

When the Mach line from 0_0 cuts the inboard but not the outboard edge of the port control, that is, when the port control is cdd′ c′ (Fig. 10), then it is evident that equation (58) is amended to

$$-C_H = \frac{\xi c_f}{s(\eta_0 - \eta_1)} \left[\chi - 2f(0, \beta) + 2f\left(\frac{\eta_0 - \eta_1}{\varepsilon}, \beta\right) + f\left(\frac{2\eta_1}{\varepsilon}, \beta\right) - 2f\left(\frac{\eta_0 + \eta_1}{\varepsilon}, \beta\right)\right]. \quad .. \quad .. \quad .. \quad .. \quad .. \quad (59)$$

Finally when the Mach line from 0_0 cuts the outboard edge of the port control, that is, when the port control takes up the position dee' d' (Fig. 10), then it is easily seen the term $f(2\eta_0/\varepsilon, \beta)$ must be added to χ in equation (59) to give

$$-C_H = \frac{\xi c_f}{s(\eta_0 - \eta_1)}\left[\chi - 2f(0, \beta) + 2f\left(\frac{\eta_0 - \eta_1}{\varepsilon}, \beta\right)\right.$$
$$\left. + f\left(\frac{2\eta_1}{\varepsilon}, \beta\right) - 2f\left(\frac{\eta_0 + \eta_1}{\varepsilon}, \beta\right) + f\left(\frac{2\eta_0}{\varepsilon}, \beta\right)\right]. \quad .. \quad .. \quad .. \quad (60)$$

It can readily be shown that as $\eta_0 - \eta_1 \to 0$, the expression in the square brackets in equation (60) is $0(\eta_0 - \eta_1)^2$, so that $-C_H \to 0$ as $\eta_0 - \eta_1 \to 0$.

Since $f(\tau, \beta) = 0$ when $\tau \geqslant 1$, equation (60) reduces to equation (59) when $2\eta_0 \geqslant \varepsilon$, to equation (58) when $2\eta_0 \geqslant \varepsilon$, $(\eta_0 + \eta_1) \geqslant \varepsilon$ and to equation (57) when in addition $2\eta_1 \geqslant \varepsilon$. Furthermore, when $\eta_0 - \eta_1 \geqslant \varepsilon$ and consequently $\eta_0 + \eta_1 \geqslant \eta_0 \geqslant \varepsilon$, equation (60) reduces to equation (56). Equation (60) is therefore valid for $0 \leqslant \eta_1 \leqslant \eta_0 \leqslant (1 - \varepsilon)$. Thus the lift, pitching-moment and hinge-moment coefficients for $0 \leqslant \eta_1 \leqslant \eta_0 \leqslant (1 - \varepsilon)$ are given by equations (50), (51) and (60), where χ and the function $f(\tau, \beta)$ are given by equations (37), (52), (53) and equations (46), (47) respectively.

4.5. *Controls with η_0 or η_1 in the Range* $(1 - \varepsilon) < \eta \leqslant (1 - \frac{1}{2}\varepsilon)$.—Consider first an outboard control with $(1 - \varepsilon) < \eta_1 \leqslant (1 - \frac{1}{2}\varepsilon)$, shown in Fig. 5. The expression for the new loading function, F_E, is derived in Appendix A. The loading $F_B + F_D - F_A$ in Fig. 5 is deduced in a similar manner to equation (44), the loading in region R_5 of Fig. 7.

To evaluate the lift and moment it is convenient to start with the fictitious loading distribution of Fig. 11, which is conctructed so that the integrals $\iint F$, $\iint XF$ are formally equivalent to those for the flow represented in Fig. 7. It is then necessary simply to add to this the loading in Fig. 12, which represents the difference between the distributions of Figs. 5 and 11. It is supposed that the Mach line from 0_1 does not cut the port tip, *i.e.*, that $\eta_1 \geqslant (\varepsilon - 1)$.

The lift coefficient corresponding to Fig. 5 is obtained by adding to equation (36) the increment

$$\Delta C_L = \frac{8}{\pi}\xi\frac{C_f^2}{s\bar{c}}\left[\iint_{\Delta_1}(F_A - F_C)\,dX\,dY_1 + \iint_{\Delta_2} F_E^*\,dX\,dY_1\right], \quad .. \quad .. \quad (61)$$

where $F_E^* = F_E + F_A - F_B - F_C$. It is easily verified from equations (15), (28) and (31) that $F_A(X) - F_C(X, Y_1) \equiv F_D(X, -Y_1)$.

Hence the first integral in equation (61) becomes

$$\iint_{\Delta_1}(F_A - F_C)\,dX\,dY_1 = \iint_{\Delta_4} F_D(X, Y_1)\,dX\,dY_1.$$

From equations (15), (24), (28) and (A.5),

$$F_E^* = F_E + F_A - F_B - F_C$$
$$= \left[\sin^{-1}\left(\frac{X - Y_1}{2X}\right)^{1/2} - \sin^{-1}\left(\frac{m_1 - Y_1}{X}\right)^{1/2}\right]\left\{1 + i\lambda X\left(\beta - \frac{1}{\beta}\right)\right\}$$
$$+ 2i\lambda\beta(m_1 - Y_1)^{1/2}\{m_1^{1/2} - (X + Y_1 - m_1)^{1/2}\}. \quad .. \quad .. \quad .. \quad (62)$$

It is easily seen from Fig. 12 that

$$\iint_{\Delta_4} F_D\,dX\,dY_1 + \iint_{\Delta_2} F_E^*\,dX\,dY_1 = \int_{m_1}^{l} dX\int_{-X}^{-m_1} F_D\,dY_1 + \int_{m_1}^{l} dX\int_{2m_1 - X}^{m_1} F_E^*\,dY_1,$$

where $l = 1/\beta$ and $m_1 = s(1 - \eta_1)/c_f$. When equations (36) and (61) are added together, for an outboard control with $(1 - \varepsilon) < \eta_1 \leqslant (1 - \frac{1}{2}\varepsilon)$

$$C_L = \frac{\xi c_f^2}{s\bar{c}}\left[\left(-\frac{1}{\beta^2} + i\lambda\frac{2}{3\beta^4}\right) + 2\tau_1\left\{\frac{2}{\beta^2} + i\lambda\left(\frac{1}{\beta^2} - \frac{1}{\beta^4}\right)\right\}\right] + \Delta C_L , \quad . . \quad . . \quad (63)$$

where

$$\Delta C_L = \frac{8}{\pi}\frac{\xi c_f^2}{s\bar{c}}\left[\frac{1}{4\beta^2}\{\tau_1^{1/2}(1 - \tau_1)^{1/2}(1 + 2\tau_1) + (1 - 4\tau_1)\sin^{-1}(1 - \tau_1)^{1/2}\}\right.$$

$$+ \frac{i\lambda}{6\beta^2}\{\tau_1^{1/2}(1 - \tau_1)^{1/2}\tau_1(5 - 2\tau_1) - 3\tau_1\sin^{-1}(1 - \tau_1)^{1/2}\}$$

$$\left. - \frac{i\lambda}{18\beta^4}\{\tau_1^{1/2}(1 - \tau_1)^{1/2}(3 + \tau_1 + 2\tau_1^2) + 3(1 - 3\tau_1)\sin^{-1}(1 - \tau_1)^{1/2}\}\right]$$

and $$\tau_1 = m_1/l = (1 - \eta_1)/\varepsilon .$$

Similarly the increment to the pitching-moment coefficient as given in equation (42) is

$$-\frac{8}{\pi}\frac{\xi c_f^3}{s\bar{c}^2}\beta\left[\iint_{\Delta_1} XF_D\, dX\, dY_1 + \iint_{\Delta_2} XF_E^*\, dX\, dY_1\right].$$

The first integral is equivalent to equation (46), when the non-dimensional distance $2(m - m_1) = 2s\eta_1/c_f$ in Fig. 8 is replaced by $m_1 = s(1 - \eta_1)/c_f$ in Fig. 12, and contributes a term

$$\frac{\pi}{8\beta}f\left(\frac{1 - \eta_1}{\varepsilon}, \beta\right) = \frac{\pi}{8\beta}f(\tau_1, \beta) .$$

The second integral plays a similar rôle, so that it is convenient to introduce another function

$$g(\tau_1, \beta) = \frac{8\beta}{\pi}\iint_{\Delta_2} XF_E^*\, dX\, dY_1 , \quad . . \quad . . \quad . . \quad . . \quad . . \quad . . \quad . . \quad (64)$$

when $1 - \eta_1 \leqslant \varepsilon$ (*i.e.*, when $\tau_1 \leqslant 1$), where F_E^* is given in equation (62). Like the function $f(\tau, \beta)$, $g(\tau_1, \beta)$ is defined to vanish when $1 - \eta_1 > \varepsilon$ (*i.e.*, when $\tau_1 > 1$).

The moment coefficient for $(1 - \varepsilon) < \eta_1 \leqslant (1 - \frac{1}{2}\varepsilon)$ is therefore given by

$$-C_m = \frac{\xi c_f^3}{s\bar{c}^2}\left[\left(-\frac{2}{3\beta^2} + i\lambda\frac{1}{2\beta^4}\right) + 2\tau_1\left\{\frac{1}{\beta^2} + i\lambda\frac{2}{3}\left(\frac{1}{\beta^2} - \frac{1}{\beta^4}\right)\right\} + f(\tau_1, \beta) + g(\tau_1, \beta)\right] . \quad . . \quad (65)$$

From equations (62) and (64) it can be shown that

$$g(\tau_1, \beta) = \frac{2}{9\pi}\left[\frac{1}{\beta^2}\{2\tau_1^{1/2}(1 - \tau_1)^{1/2}(3 + \tau_1 + 2\tau_1^2) - 3(1 - \tau_1^2)^{1/2}(2 + \tau_1^2)\right.$$

$$+ 6(1 - 3\tau_1)\cos^{-1}\tau_1^{1/2} + 9\tau_1\cos^{-1}\tau_1\} + \frac{i\lambda}{10\beta^2}\left\{8\tau_1^{1/2}(1 - \tau_1)^{1/2}\tau_1(21 - 2\tau_1 - 4\tau_1^2)\right.$$

$$+ 15\tau_1^2(1 - \tau_1^2)^{1/2} - 120\tau_1\cos^{-1}\tau_1^{1/2} + 60\tau_1\cos^{-1}\tau_1$$

$$\left. - 15\tau_1^2(6 - \tau_1^2)\cosh^{-1}\left(\frac{1}{\tau_1}\right)\right\} - \frac{i\lambda}{20\beta^4}\left\{2\tau_1^{1/2}(1 - \tau_1)^{1/2}(45 + 6\tau_1 + 8\tau_1^2 + 16\tau_1^3)\right.$$

$$- 15(1 - \tau_1^2)^{1/2}(6 + \tau_1^2) + 30(3 - 8\tau_1)\cos^{-1}\tau_1^{1/2} + 120\tau_1\cos^{-1}\tau_1$$

$$\left. - 15\tau_1^4\cosh^{-1}\left(\frac{1}{\tau_1}\right)\right\}\Bigg] \quad . . \quad . . \quad . . \quad . . \quad . . \quad . . \quad . . \quad . . \quad (66)$$

$$\text{for } \tau_1 \leqslant 1$$

$$= 0 \qquad \text{for } \tau_1 > 1 .$$

The hinge moment is evaluated by subtracting from the pitching-moment integrals corresponding to equation (65) the integrals over the triangular region whose vertices are $(X, Y_1) = (0, 0)$, $(l, 0)$ and $(l, -l)$ in Fig. 5,

$$\left.\begin{aligned} \iint_D XF_D\, dX\, dY_1 &= \frac{\pi}{8\beta} f(0, \beta) \\ \text{and} \qquad \iint_{A_3} X(F_B - F_A)\, dX\, dY_1 &= \int_{m_1}^{l} X\, dX \int_{-(X-m_1)}^{0} (F_B - F_A)\, dY_1 \end{aligned}\right\} \quad .. \quad .. \quad (67)$$

where $l = 1/\beta$, $m_1 = \tau_1/\beta$.

By equations (15) and (24) the second integral in equation (67) is evaluated to be

$$\begin{aligned} &- \frac{1}{18\beta^3}\{\tau_1^{1/2}(1-\tau_1)^{1/2}(3+\tau_1+2\tau_1^2) + 3(1-3\tau_1)\cos^{-1}\tau_1^{1/2}\} \\ &- \frac{i\lambda}{180\beta^3}\{\tau_1^{1/2}(1-\tau_1)^{1/2}(45-78\tau_1+16\tau_1^2+32\tau_1^3) + 15(3-4\tau_1)\cos^{-1}\tau_1^{1/2}\} \\ &+ \frac{i\lambda}{360\beta^5}\{\tau_1^{1/2}(1-\tau_1)^{1/2}(45+6\tau_1+8\tau_1^2+16\tau_1^3) + 15(3-8\tau_1)\cos^{-1}\tau_1^{1/2}\}. \end{aligned}$$

From this result and equations (65) and (67) an expression for the hinge moment is obtained. However, the possible interference of the port control has not been taken into account. So the quantity $[(\xi c_f)/\{s(1-\eta_1)\}]f[(2\eta_1/\varepsilon), \beta]$ must be included as was done in deriving equation (56) from equation (55). This gives

$$\begin{aligned} -C_H = \frac{\xi c_f}{s(1-\eta_1)}\Bigg[&\left(-\frac{2}{3\beta^2} + i\lambda\frac{1}{2\beta^4}\right) + 2\tau_1\left\{\frac{1}{\beta^2} + i\lambda\tfrac{2}{3}\left(\frac{1}{\beta^2}-\frac{1}{\beta^4}\right)\right\} \\ &+ f(\tau_1, \beta) + g(\tau_1, \beta) - f(0, \beta) + f\left(\frac{2\eta_1}{\varepsilon}, \beta\right) \\ &+ \frac{4}{9\pi\beta^2}\{\tau_1^{1/2}(1-\tau_1)^{1/2}(3+\tau_1+2\tau_1^2) + 3(1-3\tau_1)\cos^{-1}\tau_1^{1/2}\} \\ &+ \frac{2i\lambda}{45\pi\beta^2}\{\tau_1^{1/2}(1-\tau_1)^{1/2}(45-78\tau_1+16\tau_1^2+32\tau_1^3) + 15(3-4\tau_1)\cos^{-1}\tau_1^{1/2}\} \\ &- \frac{i\lambda}{45\beta^4\pi}\{\tau_1^{1/2}(1-\tau_1)^{1/2}(45+6\tau_1+8\tau_1^2+16\tau_1^3) + 15(3-8\tau_1)\cos^{-1}\tau_1^{1/2}\}\Bigg], \end{aligned} \quad (68)$$

where $\tau_1 = (1-\eta_1)/\varepsilon$. Thus, for an outboard control, the lift, pitching moment and hinge moment are given by equations (63), (65) and (68), provided that $(1-\varepsilon) < \eta_1 \leqslant (1-\frac{1}{2}\varepsilon)$ and $\eta_1 \geqslant (\varepsilon - 1)$, the latter condition being automatically satisfied when $\varepsilon < 1$.

Now consider a general control with $0 \leqslant \eta_1 \leqslant \eta_0 \leqslant (1-\frac{1}{2}\varepsilon)$, the condition $\eta_1 \geqslant (\varepsilon - 1)$ being satisfied. The case where $\eta_0 \leqslant (1-\varepsilon)$ has been treated in section 4.4. The expressions for the lift and pitching moment are obtained by the superposition of flows as in section 4.4. Thus when $0 \leqslant \eta_1 \leqslant (1-\varepsilon)$:

$$C_L = [\text{R.H.S. of equation (36)}] - [\text{R.H.S. of equation (63) with } \tau_1 \text{ replaced by } \tau_0], \quad (69)$$

where $\tau_0 = (1-\eta_0)/\varepsilon$. Similarly when $(1-\varepsilon) \leqslant \eta_1 \leqslant \eta_0 \leqslant (1-\frac{1}{2}\varepsilon)$:

$$C_L = [\text{R.H.S. of equation (63)}] - [\text{R.H.S. of equation (63) with } \tau_1 \text{ replaced by } \tau_0]. \quad (70)$$

In the expression for the pitching moment in equation (65) the functions $f(\tau_1, \beta)$, $g(\tau_1, \beta)$ vanish when $\eta_1 \leqslant (1-\varepsilon)$, so that equation (65) reduces to equation (42) and is therefore valid for $0 \leqslant \eta_1 \leqslant (1-\frac{1}{2}\varepsilon)$, $\eta_0 = 1$. This result enables the pitching moment for a general control to be written as

$$-C_m = [\text{R.H.S. of equation (65)}] - [\text{R.H.S. of equation (65) with } \tau_1 \text{ replaced by } \tau_0]. \quad (71)$$

In section 4.4 it is shown that the hinge moment is given by equation (60) for $0 \leqslant \eta_1 \leqslant \eta_0 \leqslant (1 - \varepsilon)$ for a general control but when $0 \leqslant \eta_1 \leqslant \eta_0 \leqslant (1 - \frac{1}{2}\varepsilon)$ the flow over the control surface experiences no interference from the tip so that equation (60) remains valid.

4.6. *Summary of Aerodynamic Coefficients.*—To complete the investigation it would be necessary to consider controls with η_1 or η_0 in the range $(1 - \frac{1}{2}\varepsilon) < \eta \leqslant 1$. Only one new loading function F_F is introduced; this is derived in Appendix B. The calculation of the lift, pitching moment and hinge moment is similar to that in section 4.5 and is omitted as it is not of much practical importance.

To summarise, expressions for the lift, pitching moment and hinge moment have been obtained, which cover the general case of Fig. 1 with three restrictions:

(*a*) $\varepsilon \leqslant 1$ (so that Mach line from inboard edge of starboard control cannot cut the port tip)

(*b*) $\eta_1 \leqslant (1 - \frac{1}{2}\varepsilon)$

(*c*) either $\eta_0 \leqslant (1 - \frac{1}{2}\varepsilon)$ or $\eta_0 = 1$.

The individual expressions only apply when further restrictions on η_0 or η_1 are made. The following table lists the appropriate equation numbers:

η_0	η_1	C_L	$-C_m$	$-C_H$
$0 \leqslant \eta_0 \leqslant (1 - \varepsilon)$	$0 \leqslant \eta_1 \leqslant \eta_0$	50	51	60†
$(1 - \varepsilon) < \eta_0 \leqslant (1 - \frac{1}{2}\varepsilon)$	$0 \leqslant \eta_1 \leqslant (1 - \varepsilon)$	69	71†	60†
$(1 - \varepsilon) < \eta_0 \leqslant (1 - \frac{1}{2}\varepsilon)$	$(1 - \varepsilon) < \eta_1 \leqslant \eta_0$	70	71	60†
$\eta_0 = 1$	$0 \leqslant \eta_1 \leqslant (1 - \varepsilon)$	36	42	49†
$\eta_0 = 1$	$(1 - \varepsilon) < \eta_1 \leqslant (1 - \frac{1}{2}\varepsilon)$	63	65	68

5. *Derivatives for a Cropped Delta Wing.*—Each aerodynamic coefficient may be split uniquely into two parts, *viz.*,

$$\left.\begin{aligned} C_L &= -2z_\xi\xi - 2z_{\dot\xi}\left(\frac{\dot\xi\bar c}{V}\right) \\ (C_m)_0 &= 2m_\xi\xi + 2m_{\dot\xi}\left(\frac{\dot\xi\bar c}{V}\right) \\ C_H &= 2h_\xi\xi + 2h_{\dot\xi}\left(\frac{\dot\xi\bar c}{V}\right) \end{aligned}\right\}, \qquad \ldots\ \ldots\ \ldots\ \ldots\ \ldots\ \ldots \quad (72)$$

where $\dot\xi = d\xi/dt$ and the real coefficients, z_ξ, $z_{\dot\xi}$, m_ξ, $m_{\dot\xi}$, h_ξ, $h_{\dot\xi}$, are the required control derivatives.

The moment in the second equation will be taken about the pitching axis through the apex of the wing so that the moment coefficient there is equal to

$$(C_m)_0 = C_m - \left(\frac{c_0 - c_f}{\bar c}\right) C_L ,$$

where C_m is taken about the hinge line. Then the above equations may be written

$$\left.\begin{aligned} C_L &= -2z_\xi\xi - 2z_{\dot\xi}\left(\frac{\dot\xi\bar c}{V}\right) \\ C_m &= 2\left\{m_\xi - \left(\frac{c_0 - c_f}{\bar c}\right) z_\xi\right\}\xi + 2\left\{m_{\dot\xi} - \left(\frac{c_0 - c_f}{\bar c}\right) z_{\dot\xi}\right\}\left(\frac{\dot\xi\bar c}{V}\right) \\ C_H &= 2h_\xi\xi + 2h_{\dot\xi}\left(\frac{\dot\xi\bar c}{V}\right) \end{aligned}\right\}, \qquad \ldots \quad (73)$$

whence the control derivatives may be evaluated from the various expressions for C_L, C_m and C_H summarised in section 4.6. However, only the cases of an outboard control when $0 \leqslant \eta_1 \leqslant (1 - \frac{1}{2}\varepsilon)$ and for an inboard control when $0 \leqslant \eta_0 \leqslant (1 - \frac{1}{2}\varepsilon)$ will be dealt with here.

† Indicates that in these equations terms in $f(\tau, \beta)$, $g(\tau, \beta)$ are zero when $\tau \geqslant 1$.

It is convenient at this stage to split the functions $f(\tau, \beta)$, $g(\tau, \beta)$ into their real and imaginary parts

$$\left.\begin{aligned} f(\tau, \beta) &= f_r(\tau, \beta) + i\lambda f_i(\tau, \beta) \\ g(\tau, \beta) &= g_r(\tau, \beta) + i\lambda g_i(\tau, \beta) \end{aligned}\right\} \quad .. \quad .. \quad .. \quad .. \quad .. \quad .. \quad (74)$$

These are identically zero for $\tau \geqslant 1$.

Consider first an outboard control when $(1 - \varepsilon) < \eta_1 \leqslant (1 - \frac{1}{2}\varepsilon)$. From equation (73) with the values of the aerodynamic coefficients given by equations (63), (65) and (68) and using equations (74) it is found that

$$\left.\begin{aligned}
-z_\xi &= \frac{c_f^2}{2s\bar{c}\beta^2}(4\tau_1 - 1) + \frac{c_f^2}{\pi s\bar{c}\beta^2}[\tau_1^{1/2}(1-\tau_1)^{1/2}(1+2\tau_1) + (1-4\tau_1)\cos^{-1}\tau_1^{1/2}] \\
-z_{\dot\xi} &= \frac{c_f^3}{s\bar{c}^2\beta^4}\{\tfrac{1}{3} + \tau_1(\beta^2 - 1)\} - \frac{2c_f^3}{9\pi s\bar{c}^2\beta^4}[\tau_1^{1/2}(1-\tau_1)^{1/2}(3+\tau_1+2\tau_1^2) \\
&\quad + 3(1-3\tau_1)\cos^{-1}\tau_1^{1/2} - 3\beta^2\tau_1\{\tau_1^{1/2}(1-\tau_1)^{1/2}(5-2\tau_1) - 3\cos^{-1}\tau_1^{1/2}\}] \\
-m_\xi &= \frac{c_f^3}{2s\bar{c}^2\beta^2}\left\{(\tfrac{1}{3} - 2\tau_1) + \frac{c_0}{c_f}(4\tau_1 - 1)\right\} + \frac{c_f^3}{2s\bar{c}^2}\left[f_r(\tau_1, \beta) + g_r(\tau_1, \beta)\right. \\
&\quad \left. + \frac{2}{\pi\beta^2}\left(\frac{c_0}{c_f} - 1\right)\{\tau_1^{1/2}(1-\tau_1)^{1/2}(1+2\tau_1) + (1-4\tau_1)\cos^{-1}\tau_1^{1/2}\}\right] \\
-m_{\dot\xi} &= \frac{c_f^4}{2s\bar{c}^3\beta^4}\left\{\tfrac{1}{6}(-1 + 4\tau_1 - 4\tau_1\beta^2) + \tfrac{2}{3}\frac{c_0}{c_f}(1 - 3\tau_1 + 3\tau_1\beta^2)\right\} \\
&\quad + \frac{c_f^4}{2s\bar{c}^3}\left[f_i(\tau_1, \beta) + g_i(\tau_1, \beta) - \frac{4}{9\pi\beta^4}\left(\frac{c_0}{c_f} - 1\right)\{\tau_1^{1/2}(1-\tau_1)^{1/2}(3+\tau_1+2\tau_1^2)\right. \\
&\quad + 3(1-3\tau_1)\cos^{-1}\tau_1^{1/2}\} \\
&\quad \left. + \frac{4}{3\pi\beta^2}\left(\frac{c_0}{c_f} - 1\right)\tau_1\{\tau_1^{1/2}(1-\tau_1)^{1/2}(5-2\tau_1) - 3\cos^{-1}\tau_1^{1/2}\}\right] \\
-h_\xi &= \frac{c_f}{2s(1-\eta_1)\beta^2}\left\{2\tau_1 - \tfrac{2}{3}\left(1 + \frac{2}{\pi}\right) + \beta^2 f_r\left(\frac{2\eta_1}{\varepsilon}, \beta\right)\right\} + \frac{c_f}{2s(1-\eta_1)}\left[f_r(\tau_1, \beta)\right. \\
&\quad \left. + g_r(\tau_1, \beta) + \frac{4}{9\pi\beta^2}\{\tau_1^{1/2}(1-\tau_1)^{1/2}(3+\tau_1+2\tau_1^2) + 3(1-3\tau_1)\cos^{-1}\tau_1^{1/2}\}\right] \\
-h_{\dot\xi} &= \frac{c_f^2}{2s\bar{c}(1-\eta_1)\beta^4}\left\{\tfrac{1}{2}\left(1 + \frac{2}{\pi}\right) + \tfrac{4}{3}\tau_1(\beta^2 - 1) + \beta^4 f_i\left(\frac{2\eta_1}{\varepsilon}, \beta\right)\right\} \\
&\quad + \frac{c_f^2}{2s\bar{c}(1-\eta_1)}\left[f_i(\tau_1, \beta) + g_i(\tau_1, \beta)\right. \\
&\quad - \frac{1}{45\pi\beta^4}\{\tau_1^{1/2}(1-\tau_1)^{1/2}(45 + 6\tau_1 + 8\tau_1^2 + 16\tau_1^3) + 15(3 - 8\tau_1)\cos^{-1}\tau_1^{1/2}\} \\
&\quad + \frac{2}{45\pi\beta^2}\{\tau_1^{1/2}(1-\tau_1)^{1/2}(45 - 78\tau_1 + 16\tau_1^2 + 32\tau_1^3) \\
&\quad \left. + 15(3 - 4\tau_1)\cos^{-1}\tau_1^{1/2}\}\right]
\end{aligned}\right\}, \quad (75)$$

where $\tau_1 = (1 - \eta_1)/\varepsilon$.

These results hold for $(1 - \varepsilon) < \eta_1 \leqslant (1 - \frac{1}{2}\varepsilon)$. The derivatives for $0 \leqslant \eta_1 \leqslant (1 - \varepsilon)$ are given by equation (75) if the terms in the square brackets are omitted.

The derivatives for an inboard control when $(1 - \varepsilon) < \eta_0 \leqslant (1 - \frac{1}{2}\varepsilon)$ are found in a similar manner. The aerodynamic coefficients in this case are given in equations (69), (71), (60) with $\eta_1 = 0$. This leads to

$$
\left.
\begin{aligned}
-z_\xi &= \eta_0 \frac{2c_f}{\bar{c}\beta} - \frac{c_f^2}{\pi s\bar{c}\beta^2}\left[\tau_0^{1/2}(1-\tau_0)^{1/2}(1+2\tau_0) + (1-4\tau_0)\cos^{-1}\tau_0^{1/2}\right] \\
-z_{\dot\xi} &= \eta_0 \frac{c_f^2}{\bar{c}^2}\left(\frac{1}{\beta} - \frac{1}{\beta^3}\right) + \frac{2}{9\pi\beta^4}\frac{c_f^3}{s\bar{c}^2}\left[\tau_0^{1/2}(1-\tau_0)^{1/2}(3+\tau_0+2\tau_0^2)\right. \\
&\quad \left. + 3(1-3\tau_0)\cos^{-1}\tau_0^{1/2} - 3\beta^2\tau_0\{\tau_0^{1/2}(1-\tau_0)^{1/2}(5-2\tau_0) - 3\cos^{-1}\tau_0^{1/2}\}\right] \\
-m_\xi &= \eta_0 \frac{c_f^2}{\bar{c}^2}\left(2\frac{c_0}{c_f} - 1\right)\frac{1}{\beta} - \frac{c_f^3}{2s\bar{c}^2}\left[f_r(\tau_0,\beta) + g_r(\tau_0,\beta)\right. \\
&\quad \left. + \frac{2}{\pi\beta^2}\left(\frac{c_0}{c_f} - 1\right)\{\tau_0^{1/2}(1-\tau_0)^{1/2}(1+2\tau_0) + (1-4\tau_0)\cos^{-1}\tau_0^{1/2}\}\right] \\
-m_{\dot\xi} &= \eta_0 \frac{c_f^3}{\bar{c}^3}\left(\frac{c_0}{c_f} - \tfrac{1}{3}\right)\left(\frac{1}{\beta} - \frac{1}{\beta^3}\right) - \frac{c_f^4}{2s\bar{c}^3}\left[f_i(\tau_0,\beta) + g_i(\tau_0,\beta)\right. \\
&\quad + \frac{4}{9\pi\beta^4}\left(1 - \frac{c_0}{c_f}\right)\{\tau_0^{1/2}(1-\tau_0)^{1/2}(3+\tau_0+2\tau_0^2) + 3(1-3\tau_0)\cos^{-1}\tau_0^{1/2}\} \\
&\quad \left. - \frac{4}{3\pi\beta^2}\left(1 - \frac{c_0}{c_f}\right)\tau_0\{\tau_0^{1/2}(1-\tau_0)^{1/2}(5-2\tau_0) - 3\cos^{-1}\tau_0^{1/2}\}\right] \\
-h_\xi &= \frac{c_f}{2s\eta_0}\left\{\eta_0\frac{2s}{c_f}\frac{1}{\beta} - f_r(0,\beta) + f_r\left(\frac{2\eta_0}{\varepsilon},\beta\right)\right\} \\
-h_{\dot\xi} &= \frac{c_f^2}{2s\bar{c}\eta_0}\left\{\eta_0\frac{4s}{3c_f}\left(\frac{1}{\beta} - \frac{1}{\beta^3}\right) - f_i(0,\beta) + f_i\left(\frac{2\eta_0}{\varepsilon},\beta\right)\right\}
\end{aligned}
\right\}, \quad \ldots \quad (76)
$$

where

$$\tau_0 = (1 - \eta_0)/\varepsilon .$$

These formulae also give the derivatives for $0 \leqslant \eta_0 \leqslant (1 - \varepsilon)$ if the terms in the square brackets are omitted.

The functions f_r, f_i, g_r, g_i defined in equation (74) are tabulated for ranges of values of $M = \sqrt{(\beta^2 + 1)}$ and τ in Tables 1 and 2. Whereas f_r and f_i are required throughout the range $0 \leqslant \tau \leqslant 1$, g_r and g_i are not required when $0 \leqslant \tau \leqslant 0{\cdot}5$ since $\tau_0 = (1 - \eta_0)/\varepsilon$ and $\tau_1 = (1 - \eta_1)/\varepsilon$ are not considered in this range. Table 2 is therefore restricted to $\tau = 0{\cdot}5\ (0{\cdot}1)\ 1{\cdot}0$.

6. *Discussion of Results.*—The derivatives given in section 5 for inboard and outboard controls are tabulated for a cropped delta wing (Fig. 1) of aspect ratio 1·8 and taper ratio 1/7. For convenience the auxiliary functions f_r, f_i, g_r, g_i are given in Tables 1 and 2 for various values of their arguments. The lift and pitching-moment derivatives from equations (75) and (76) are given in Table 3 and the hinge-moment derivatives in Table 4.

The stiffness or steady derivatives are plotted against the span of inboard and outboard controls for Mach numbers $M = 1{\cdot}1$, $1{\cdot}2$, $1{\cdot}4$, $1{\cdot}6$, $2{\cdot}0$ in Fig. 13 while the damping or out-of-phase derivatives are similarly plotted in Fig. 14. From Fig. 14 it is seen that $-h_{\dot\xi}$ rapidly decreases so as to become increasingly unstable as the Mach number decreases below 1·4 for an outboard control, this being particularly noticeable for the larger spans. For an outboard control with η_1 in the range $0{\cdot}6 \leqslant \eta_1 \leqslant 1$ it is evident that the interference from the tip gives a stabilising effect and positive damping at these lower Mach numbers.

The variation of the derivatives with Mach number is shown in Fig. 15, a cross-plot of Figs. 13 and 14 for the particular cases of full-span, half-span inboard and half-span outboard controls. From the graph of $-h_{\xi}^{\cdot}$ it is seen that instability ($-h_{\xi}^{\cdot} < 0$) occurs below Mach numbers of 1·4, 1·35 and 1·25 for these respective controls.

Fig. 16 illustrates the variation of the hinge-moment derivatives with frequency. The results given for frequency parameters $\nu = \omega\bar{c}/V = 0{\cdot}8$, 1·6 and 2·4 are those calculated by Acum[3] (1950). From these curves it is evident that there is a negligible variation in the derivatives with frequency in the range $0 \leqslant \nu \leqslant 0{\cdot}8$ for $M > 1{\cdot}4$. For lower Mach numbers the effect of frequency becomes more pronounced, but it amounts to less than 6 per cent for $0 \leqslant \nu \leqslant 0{\cdot}4$ and $M > 1{\cdot}2$. Within these limits the present theory seems satisfactory.

Finally the variation of full-span hinge-moment derivatives with Mach number ($0 \leqslant M \leqslant 2$) is shown in Fig. 17. The subsonic points are taken from calculations by an extension of the Multhopp-Garner theory[4] (1952) and the preliminary experimental values of $-h_{\xi}^{\cdot}$ and $-h_{\dot{\xi}}$ have been obtained by Bratt of the N.P.L. The theoretical curves in the range $0{\cdot}8 < M < 1{\cdot}0$ are only speculative. In the subsonic range the theoretical and experimental values are in good agreement except near $M = 1$; this is particularly true for $-h_{\dot{\xi}}$. On the other hand there is not good agreement in the supersonic range near $M = 1$; linearized theory predicts too high a value for $-h_{\xi}^{\cdot}$ and too low a value for $-h_{\dot{\xi}}$. It is expected, however, that agreement between theory and experiment will considerably improve for higher values of Mach number.

7. *Acknowledgements.*—Most of the numerical results in this report were calculated by Mrs. J. S. Sindall and Miss S. M. Passmore.

LIST OF SYMBOLS

a		Speed of sound
$A \ldots D, G$		Areas of integration (Figs. 3, 4, 8)
c_0		Root chord
c_f		Control chord (tip chord)
$\bar{c}$		Mean chord
	$=$	$\frac{1}{2}(c_0 + c_f)$
C_H		Complex hinge-moment coefficient
	$=$	$H/\frac{1}{2}\rho_0 V^2 S_f c_f$
C_L		Complex lift coefficient
	$=$	$L/\frac{1}{2}\rho_0 V^2 S$
C_m		Complex pitching-moment coefficient
	$=$	$\mathscr{M}/\frac{1}{2}\rho_0 V^2 S\bar{c}$
f	$=$	$f_r + i\lambda f_i$ (defined by equations (46), (47))
F		Complex non-dimensional loading (equation (14))
$F_A \ldots F_F, F_E^*$		Values of F defined by equations (15), (16), (28), (31), (A.5), (B.3), (62)

g	=	$g_r + i\lambda g_i$ (given by equation (66))
h_ξ, $h_{\dot{\xi}}$		Stiffness, damping derivative of hinge moment (equation (72))
H		Complex hinge moment
K	=	$\cot\mu(1 + \sec^2\mu)$
l		Non-dimensional tip chord (*see* Fig. 3)
	=	$1/\beta$
m		Non-dimensional semi-span of wing (*see* Fig. 3)
	=	s/c_f
L		Complex lift
m_1		Non-dimensional span of outboard control (*see* Fig. 4)
	=	$s(1 - \eta_1)/c_f$
m_ξ, $m_{\dot{\xi}}$		Stiffness, damping derivative of pitching moment (equation (72))
M		Mach number of free stream
	=	V/a
$\mathscr{M}$		Complex pitching moment about hinge line (nose up)
P		Complex pressure difference across control (equation (13))
p_0		Pressure of free stream
(r, s)		Axes parallel to Mach lines (equation (7))
$R_1 \ldots R_5$		Regions of flow (*see* Fig. 7)
s		Semi-span of wing
S		Surface area of wing
	=	$2s\bar{c}$
S_f		Surface area of control
	=	$2sc_f(\eta_0 - \eta_1)$
$S_1 \ldots S_6$		Areas of integration shown in Figs. 3, 4, 5, 6
t		Time
T		Non-dimensional time
	=	Vt/c_f
V		Speed of free stream
w		Complex upward component of velocity
x, y, z		Rectangular Cartesian co-ordinates defined by Figs. 1, 2
X, Y, Z		Non-dimensional co-ordinates defined by equation (2)

LIST OF SYMBOLS—*continued*

Y_0, Y_1		Co-ordinate referred to 0_0, 0_1 as origin (*see* Fig. 9)
z_ξ, $z_{\dot{\xi}}$		Stiffness, damping derivative of lift (equation (72))
β	$=$	$\sqrt{(M^2-1)}$
$\Delta_1 \ldots \Delta_4$		Areas of integration shown in Fig. 12
ε	$=$	$c_f/\beta s = l/m$
ζ		Complex downward displacement (*see* Fig. 2)
η		Non-dimensional spanwise ordinate
	$=$	$y/s = Yc_f/s$
η_0, η_1		Value of η at outboard, inboard edge of control
λ		Frequency parameter based on control chord
	$=$	$\omega c_f/V$
μ		Mach angle
	$=$	$\sin^{-1} 1/M$
ν		Frequency parameter based on mean chord
	$=$	$\omega \bar{c}/V$
ξ, ξ_0		Complex angle, amplitude of control deflection
ρ_0		density of free stream
τ_1; τ_0	$=$	$(1-\eta_1)/\varepsilon$; $(1-\eta_0)/\varepsilon$
ϕ		Perturbation velocity potential
Φ		Time-independent complex perturbation velocity potential (equation (3))
χ		Function (equation (53))
ω		$2\pi \times$ (frequency of oscillation of control)

REFERENCES

No.	*Author*	*Title, etc.*
1	J. C. Evvard	Use of source distributions for evaluating theoretical aerodynamics of thin finite wings at supersonic speeds. N.A.C.A. Report 951. 1950.
2	W. P. Jones	Supersonic theory for oscillating wings of any plan-form. R. & M. 2655. June, 1948.
3	W. E. A. Acum	Aerodynamic forces on rectangular wings oscillating in a supersonic air stream. R. & M. 2763. August, 1950.
4	H. C. Garner	Multhopp's subsonic lifting surface theory of wings in slow pitching oscillations. R. & M. 2885. July, 1952.

APPENDIX A

Calculation of $\Phi(X, Y_1)$ in Region E

As in section 4.1, $\Phi(X, Y_1)$ in region E (Fig. 5) is given by

$$\Phi(X, Y_1) = \frac{\xi_0 V c_f}{\pi\sqrt{2}} \iint_{S_5} \frac{\left[1 + i\lambda K\left(\frac{s_0 + r_0}{\sqrt{2}}\right)\right]}{(r_1 - r_0)^{1/2}(s_1 - s_0)^{1/2}} dr_0\, ds_0\,, \qquad \ldots\ \ldots\ \ldots\ \ldots \quad (A.1)$$

where the area of integration S_5 is given by

$$r_0 \leqslant s_0 \leqslant s_1,\ s_1 - m_1\sqrt{2} \leqslant r_0 \leqslant r_1\,.$$

Hence, in region E,

$$\begin{aligned}
\Phi(X, Y_1) &= \frac{\xi_0 V c_f}{\pi\sqrt{2}} \int_{s_1 - m_1\sqrt{2}}^{r_1} dr_0 \left\{ \int_{r_0}^{s_1} \frac{\left[1 + i\lambda K\left(\frac{s_0 + r_0}{\sqrt{2}}\right)\right]}{(r_1 - r_0)^{1/2}(s_1 - s_0)^{1/2}} ds_0 \right\} \\
&= \frac{\xi_0 V c_f}{\pi\sqrt{2}} \left[\int_{s_1 - m_1\sqrt{2}}^{r_1} \frac{2(s_1 - r_0)^{1/2}}{(r_1 - r_0)^{1/2}} dr_0 \right. \\
&\quad \left. + \frac{i\lambda K}{\sqrt{2}} \int_{s_1 - m_1\sqrt{2}}^{r_1} \frac{4(s_1 - r_0)^{1/2}(s_1 + 2r_0)}{3(r_1 - r_0)^{1/2}} dr_0 \right] \qquad \ldots\ \ldots\ \ldots\ \ldots \quad (A.2) \\
&= \frac{\xi_0 V c_f}{\pi\sqrt{2}} \left[2(s_1 - r_1) \sinh^{-1}\left(\frac{r_1 - s_1 + m_1\sqrt{2}}{s_1 - r_1}\right)^{1/2} \right. \\
&\quad + 2(m_1\sqrt{2})^{1/2}(r_1 - s_1 + m_1\sqrt{2})^{1/2} \\
&\quad + \frac{i\lambda K}{\sqrt{2}} \left\{ 2(s_1^2 - r_1^2) \sinh^{-1}\left(\frac{r_1 - s_1 + m_1\sqrt{2}}{s_1 - r_1}\right)^{1/2} \right. \\
&\quad \left. \left. + 2(m_1\sqrt{2})^{1/2}(r_1 - s_1 + m_1\sqrt{2})^{1/2}\left(s_1 + r_1 - \frac{2m_1\sqrt{2}}{3}\right) \right\} \right] \\
&= \frac{V\xi_0 c_f}{\pi\sqrt{2}} \left[(2\sqrt{2}) Y_1 \sinh^{-1}\left(\frac{m_1 - Y_1}{Y_1}\right)^{1/2} + (2\sqrt{2}) m_1^{1/2}(m_1 - Y_1)^{1/2} \right. \\
&\quad \left. + \frac{i\lambda K}{\sqrt{2}} \left\{ 4XY_1 \sinh^{-1}\left(\frac{m_1 - Y_1}{Y_1}\right)^{1/2} + 4m_1^{1/2}(m_1 - Y_1)^{1/2}\left(X - \frac{2m_1}{3}\right) \right\} \right]. \qquad (A.3)
\end{aligned}$$

This gives

$$\left(\frac{\partial \Phi}{\partial X}\right)_{Z=0} = \frac{2V\xi_0 c_f}{\pi}\, i\lambda K \left[Y_1 \sinh^{-1}\left(\frac{m_1 - Y_1}{Y_1}\right)^{1/2} + m_1^{1/2}(m_1 - Y_1)^{1/2} \right]. \quad \ldots\ \ldots \quad (A.4)$$

From equations (13) and (14), (A.3) and (A.4), it is found that

$$F = F_E = 2i\lambda\beta \left[Y_1 \sinh^{-1}\left(\frac{m_1 - Y_1}{Y_1}\right)^{1/2} + m_1^{1/2}(m_1 - Y_1)^{1/2} \right]. \quad \ldots\ \ldots \quad (A.5)$$

APPENDIX B

Calculation of $\Phi(X, Y_1)$ in Region F

In region F (Fig. 6), $\Phi(X, Y_1)$ is given by equation (A.1), where the area of integration S_6 is here $r_0 \leqslant s_0 \leqslant s_1$, $s_1 - m_1\sqrt{2} \leqslant r_0 \leqslant s_1$, so that $\Phi(X, Y_1)$ is given by equation (A.2) with the upper limit, r_1, replaced by s_1.

This gives, in region F,

$$\begin{aligned}\Phi(X, Y_1) = \frac{\xi_0 V c_f}{\pi\sqrt{2}}\Bigg[&2(m_1\sqrt{2})^{1/2}(r_1 - s_1 + m_1\sqrt{2})^{1/2} \\ &- 2(r_1 - s_1)\cosh^{-1}\left(\frac{r_1 - s_1 + m_1\sqrt{2}}{r_1 - s_1}\right)^{1/2} \\ &+ \frac{i\lambda K}{\sqrt{2}}\Big\{2(s_1^2 - r_1^2)\cosh^{-1}\left(\frac{r_1 - s_1 + m_1\sqrt{2}}{r_1 - s_1}\right)^{1/2} \\ &+ 2(m_1\sqrt{2})^{1/2}(r_1 - s_1 + m_1\sqrt{2})^{1/2}(s_1 + r_1 - \tfrac{2}{3}m_1\sqrt{2})\Big\}\Bigg] \\ = \frac{V\xi_0 c_f}{\pi\sqrt{2}}\Bigg[&2\sqrt{2}Y_1\cosh^{-1}\left(\frac{Y_1 - m_1}{Y_1}\right)^{1/2} + (2\sqrt{2})m_1^{1/2}(m_1 - Y_1)^{1/2} \\ &+ \frac{i\lambda K}{\sqrt{2}}\Big\{4XY_1\cosh^{-1}\left(\frac{Y_1 - m_1}{Y_1}\right)^{1/2} + 4m_1^{1/2}(m_1 - Y_1)^{1/2}(X - \tfrac{2}{3}m_1)\Big\}\Bigg]. \quad \text{(B.1)}\end{aligned}$$

Hence

$$\left(\frac{\partial\Phi}{\partial X}\right)_{Z=0} = \frac{2V\xi_0 c_f}{\pi} i\lambda K\left[Y_1\cosh^{-1}\left(\frac{Y_1 - m_1}{Y_1}\right)^{1/2} + m_1^{1/2}(m_1 - Y_1)^{1/2}\right]. \quad \text{(B.2)}$$

From equations (13) and (14), (B.1) and (B.2), it is found that

$$F = F_F = 2i\lambda\beta\left[Y_1\cosh^{-1}\left(\frac{Y_1 - m_1}{Y_1}\right)^{1/2} + m_1^{1/2}(m_1 - Y_1)^{1/2}\right]. \quad \text{(B.3)}$$

TABLE 1

Function $f = f_r + i\lambda f_i$ for certain Mach Numbers

(a) Values of f_r

τ / M	0	0·2	0·4	0·6	0·8	0·9	1·0
1·10	2·0210	1·1895	0·5947	0·2212	0·0400	0·0072	0
1·15	1·3160	0·7746	0·3873	0·1440	0·0261	0·0047	0
1·20	0·9646	0·5677	0·2838	0·1056	0·0191	0·0034	0
1·25	0·7545	0·4441	0·2220	0·0826	0·0149	0·0027	0
1·30	0·6151	0·3620	0·1810	0·0673	0·0122	0·0022	0
1·40	0·4421	0·2602	0·1301	0·0484	0·0088	0·0016	0
1·50	0·3395	0·1998	0·0999	0·0372	0·0067	0·0012	0
1·60	0·2721	0·1601	0·0801	0·0298	0·0054	0·0010	0
1·80	0·1895	0·1115	0·0558	0·0207	0·0038	0·0007	0
2·00	0·1415	0·0833	0·0416	0·0155	0·0028	0·0005	0

(b) Values of $-f_i$

τ / M	0	0·2	0·4	0·6	0·8	0·9	1·0
1·10	7·2179	4·7850	2·6489	1·0805	0·2129	0·0396	0
1·15	3·0605	2·0964	1·1848	0·4906	0·0978	0·0183	0
1·20	1·6442	1·1641	0·6711	0·2818	0·0567	0·0107	0
1·25	1·0060	0·7364	0·4327	0·1840	0·0374	0·0071	0
1·30	0·6686	0·5061	0·3029	0·1303	0·0267	0·0051	0
1·40	0·3454	0·2798	0·1732	0·0761	0·0158	0·0030	0
1·50	0·2037	0·1766	0·1127	0·0505	0·0106	0·0020	0
1·60	0·1308	0·1213	0·0796	0·0362	0·0077	0·0015	0
1·80	0·0634	0·0673	0·0464	0·0216	0·0048	0·0009	0
2·00	0·0354	0·0428	0·0307	0·0146	0·0032	0·0006	0

TABLE 2

Function $g = g_r + i\lambda g_i$ for certain Mach Numbers

(a) Values of g_r

τ / M	0·5	0·6	0·7	0·8	0·9	1·0
1·10	0·17197	0·09751	0·04717	0·01704	0·00300	0
1·15	0·11198	0·06349	0·03072	0·01109	0·00195	0
1·20	0·08208	0·04654	0·02251	0·00813	0·00143	0
1·25	0·06420	0·03640	0·01761	0·00636	0·00112	0
1·30	0·05234	0·02968	0·01436	0·00519	0·00091	0
1·40	0·03762	0·02133	0·01032	0·00373	0·00066	0
1·50	0·02889	0·01638	0·00792	0·00286	0·00050	0
1·60	0·02315	0·01313	0·00635	0·00229	0·00040	0
1·80	0·01612	0·00914	0·00442	0·00160	0·00028	0
2·00	0·01204	0·00683	0·00330	0·00119	0·00021	0

(b) Values of $-g_i$

τ / M	0·5	0·6	0·7	0·8	0·9	1·0
1·10	0·80565	0·47732	0·24095	0·09069	0·01664	0
1·15	0·36347	0·21679	0·11009	0·04165	0·00768	0
1·20	0·20753	0·12455	0·06359	0·02417	0·00447	0
1·25	0·13481	0·08136	0·04174	0·01594	0·00296	0
1·30	0·09500	0·05764	0·02970	0·01138	0·00212	0
1·40	0·05500	0·03368	0·01749	0·00675	0·00127	0
1·50	0·03619	0·02234	0·01168	0·00453	0·00085	0
1·60	0·02581	0·01604	0·00843	0·00328	0·00062	0
1·80	0·01526	0·00958	0·00508	0·00199	0·00038	0
2·00	0·01021	0·00647	0·00345	0·00136	0·00026	0

TABLE 3

Lift and Pitching-Moment Derivatives

Inboard control $0 \leqslant \eta \leqslant \eta_0$

M	η_0	$-z_\xi$	$-m_\xi$	$-z_{\dot{\xi}}$	$-m_{\dot{\xi}}$
—	0	0	0	0	0
1·1	0·3938†	0·4297	0·6982	−0·2021	−0·3368
1·1	0·4544	0·4954	0·8051	−0·2326	−0·3877
1·1	0·5756	0·6221	1·0103	−0·2878	−0·4792
1·1	0·6968	0·7377	1·1968	−0·3315	−0·5513
1·1	1	0·9257	1·4974	−0·3818	−0·6337
1·2	0·5812†	0·4381	0·7119	−0·0697	−0·1162
1·2	0·6650	0·5002	0·8128	−0·0790	−0·1316
1·2	0·7906	0·5852	0·9500	−0·0881	−0·1465
1·2	1	0·6748	1·0933	−0·0900	−0·1494
1·4	0·7165†	0·3657	0·5941	−0·0019	−0·0032
1·4	0·7732	0·3941	0·6404	−0·0018	−0·0031
1·4	0·8583	0·4331	0·7033	−0·0005	−0·0007
1·4	1	0·4741	0·7690	+0·0036	+0·0062
1·6	0·7776†	0·3113	0·5058	0·0140	0·0233
1·6	0·8221	0·3288	0·5343	0·0149	0·0248
1·6	0·8888	0·3528	0·5730	0·0168	0·0280
1·6	1	0·3780	0·6133	0·0204	0·0340
2·0	0·8396†	0·2423	0·3939	0·0202	0·0337
2·0	0·8717	0·2515	0·4087	0·0210	0·0350
2·0	0·9198	0·2639	0·4288	0·0225	0·0374
2·0	1	0·2771	0·4498	0·0247	0·0412

† Signifies that all four derivatives are linear in η_0 from $\eta_0 = 0$ to this value. The derivatives for a general control may be obtained by superposition.

TABLE 4

Hinge-Moment Derivatives

Inboard control $0 \leqslant \eta \leqslant \eta_0$

Outboard control $\eta_1 \leqslant \eta \leqslant 1$

		Inboard control		Outboard control	
M	η_0 or η_1	$-h_\xi$	$-h_{\dot{\xi}}$	$-h_\xi$	$-h_{\dot{\xi}}$
1·1	0	0	0	1·7413	−0·9748
1·1	0·1212	0·5477	−0·0592	1·4552	−0·7400
1·1	0·2425	1·0476	−0·3652	1·2335	−0·5224
1·1	0·3031	1·2561	−0·5413	1·1471	−0·4441
1·1	0·3485	1·3768	−0·6490	1·0749	−0·3795
1·1	0·3938	1·4694	−0·7317	0·9918	−0·3053
1·1	0·4544	1·5645	−0·8166	0·8647	−0·1920
1·1	0·5756	1·6945	−0·9328	0·5840	+0·0619
1·1	0·6968	1·7793	−1·0085	0·3090	+0·3445
1·2	0	0	0	1·2972	−0·2301
1·2	0·0838	0·3794	0·0834	1·1747	−0·1850
1·2	0·1675	0·7237	0·0093	1·0971	−0·1459
1·2	0·2094	0·8679	−0·0472	1·0720	−0·1342
1·2	0·3350	1·1077	−0·1494	0·9897	−0·0991
1·2	0·4606	1·2168	−0·1958	0·8691	−0·0477
1·2	0·5812	1·2771	−0·2216	0·6852	+0·0307
1·2	0·6650	1·3061	−0·2339	0·5021	+0·1115
1·2	0·7906	1·3381	−0·2476	0·2133	+0·2847
1·4	0	0	0	0·9241	0·0118
1·4	0·0567	0·2563	0·0984	0·8724	0·0192
1·4	0·1134	0·4899	0·0938	0·8439	0·0271
1·4	0·1418	0·5876	0·0775	0·8366	0·0288
1·4	0·2835	0·8040	0·0352	0·8002	0·0359
1·4	0·4253	0·8762	0·0211	0·7458	0·0466
1·4	0·5670	0·9123	0·0141	0·6560	0·0641
1·4	0·7165	0·9349	0·0097	0·4639	0·1017
1·4	0·7732	0·9412	0·0084	0·3399	0·1287
1·4	0·8583	0·9491	0·0069	0·1443	0·2083
1·6	0	0	0	0·7413	0·0550
1·6	0·0667	0·2961	0·0971	0·7009	0·0591
1·6	0·1112	0·4607	0·0887	0·6913	0·0610
1·6	0·2446	0·6461	0·0665	0·6720	0·0634
1·6	0·3781	0·7006	0·0599	0·6444	0·0667
1·6	0·5115	0·7267	0·0568	0·6017	0·0718
1·6	0·6450	0·7420	0·0549	0·5270	0·0808
1·6	0·7776	0·7520	0·0537	0·3639	0·1004
1·6	0·8221	0·7547	0·0534	0·2666	0·1145
1·6	0·8888	0·7581	0·0530	0·1133	0·1674
2·0	0	0	0	0·5466	0·0661
2·0	0·0481	0·2139	0·0791	0·5266	0·0670
2·0	0·0802	0·3325	0·0794	0·5225	0·0676
2·0	0·2245	0·4899	0·0696	0·5123	0·0683
2·0	0·3689	0·5242	0·0675	0·4974	0·0692
2·0	0·5132	0·5392	0·0666	0·4736	0·0707
2·0	0·6736	0·5483	0·0660	0·4226	0·0739
2·0	0·8396	0·5540	0·0656	0·2624	0·0839
2·0	0·8717	0·5548	0·0656	0·1923	0·0901
2·0	0·9198	0·5560	0·0655	0·0817	0·1229

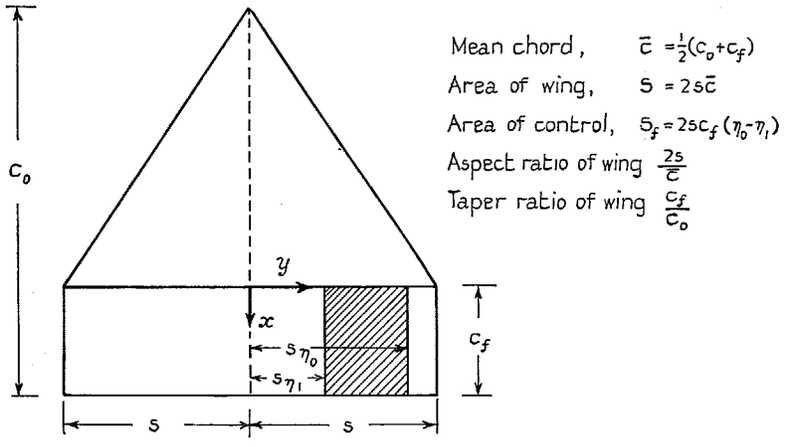

FIG 1. Plan of wing.

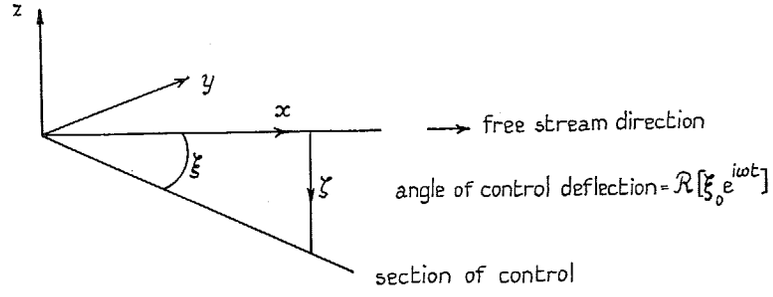

FIG. 2. Motion of control surface.

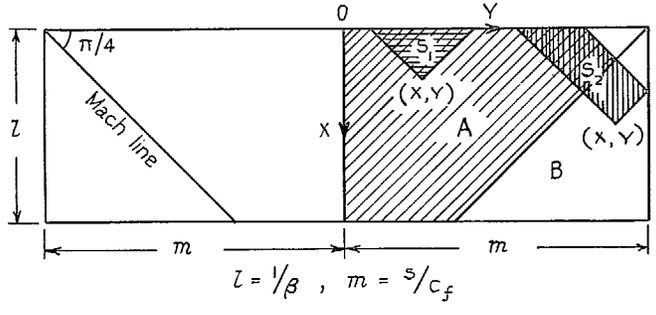

FIG. 3. ' Transform ' of full-span control.

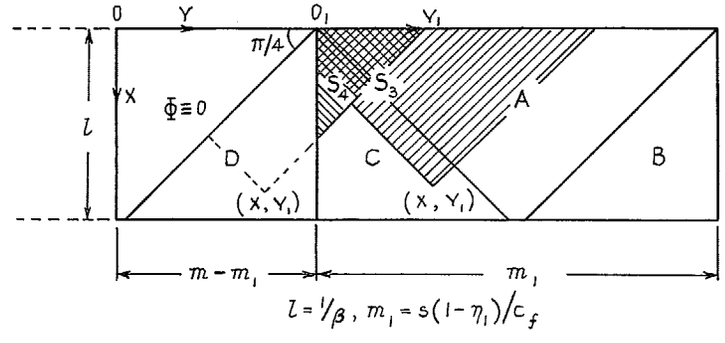

A, B, C, D denote regions in which the loading is F_A, F_B, F_C, F_D

FIG. 4. ' Transform ' of starboard outboard control.

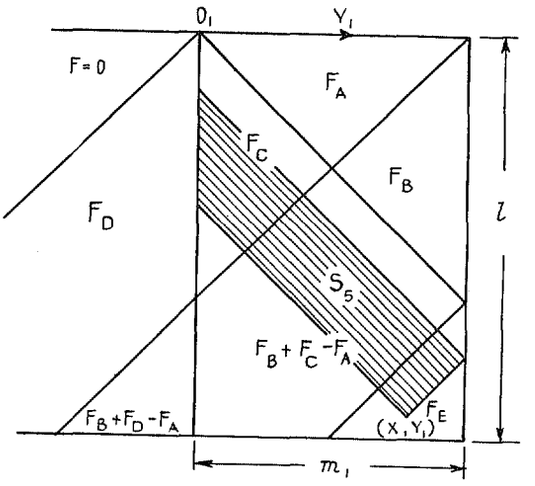

FIG. 5. Outboard control $(1 - \varepsilon) < \eta_1 \leqslant (1 - \frac{1}{2}\varepsilon)$.

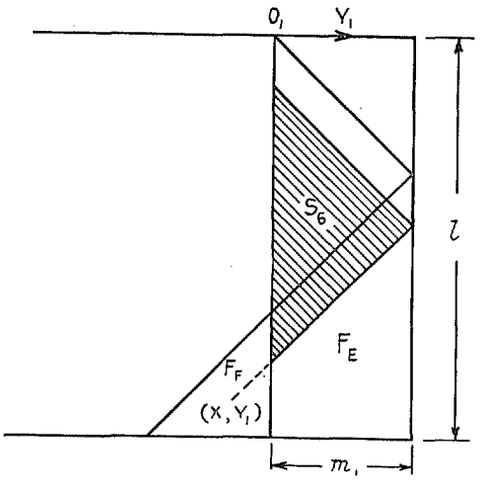

FIG. 6. Outboard control $(1 - \frac{1}{2}\varepsilon) < \eta_1 \leqslant 1$.

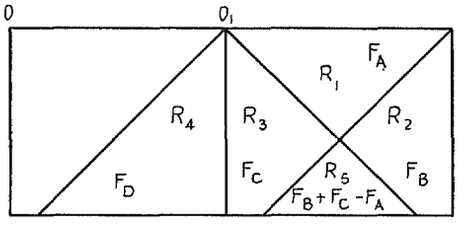

FIG. 7. Mach lines crossing on starboard outboard control.

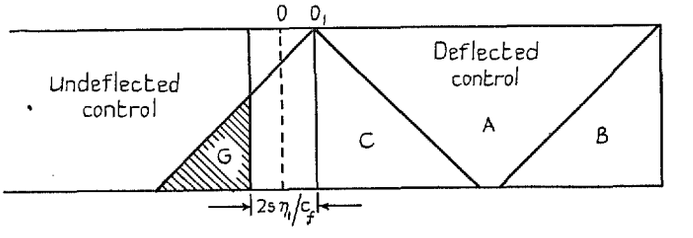

FIG. 8. Mach line crossing port control.

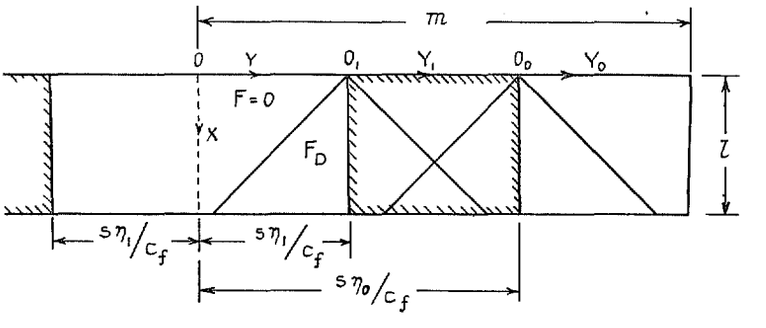

$\frac{1}{2}\epsilon \leq \eta_1 \leq \eta_0 \leq (1 - 2\epsilon)$, where $\epsilon = \frac{c_f}{\beta s} = \frac{l}{m}$

FIG. 9. Load distribution off general control $(\eta_0 - \eta_1) \geqslant \varepsilon$.

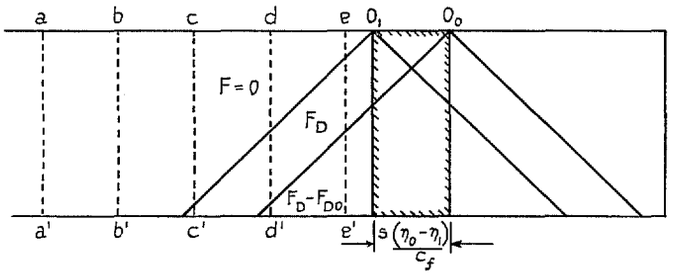

abb'a', bcc'b', cdd'c', dee'd'

FIG. 10. Various positions of port control $(\eta_0 - \eta_1) < \varepsilon$.

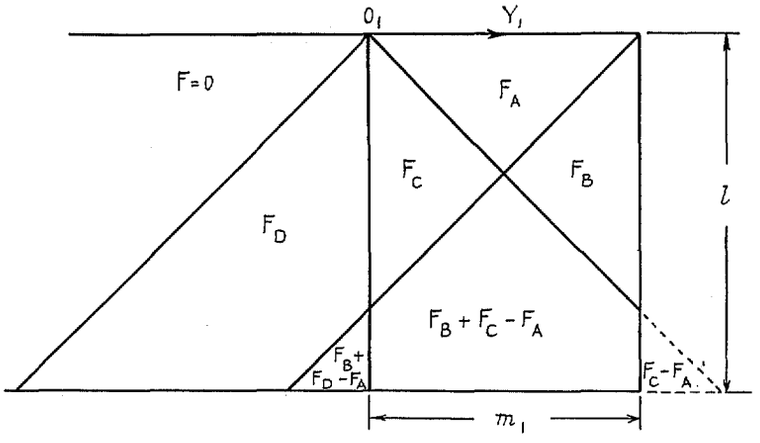

FIG. 11. Fictitious load distribution for outboard control.

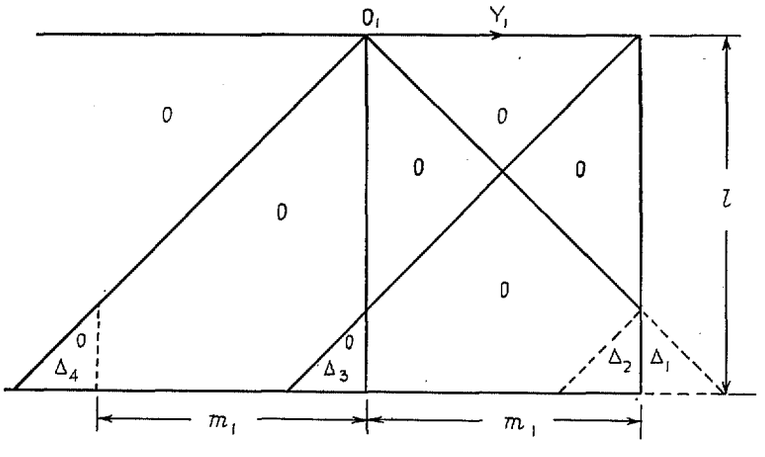

In Δ_1, $F = F_A - F_C$

In Δ_2, $F = F_E + F_A - F_B - F_C$

FIG. 12. Difference between load distributions in Figs. 5 and 11.

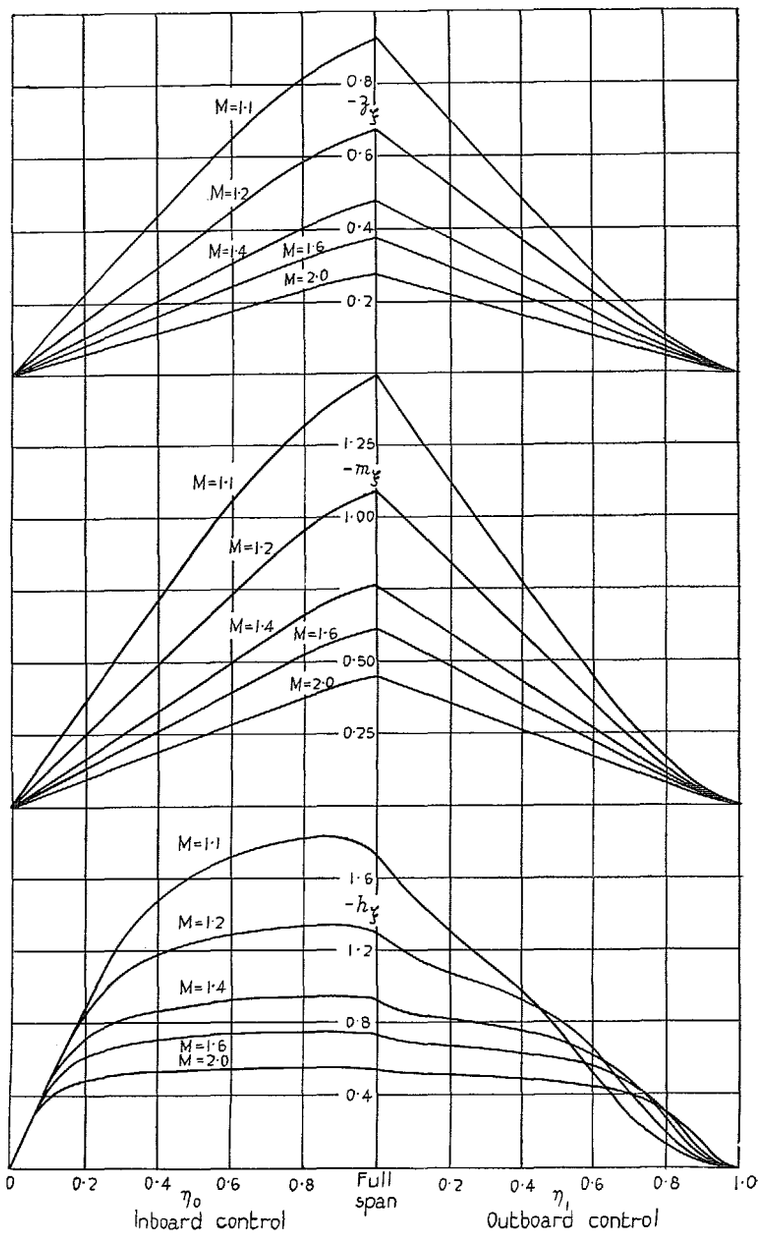

FIG. 13. Variation of stiffness derivatives with control span.

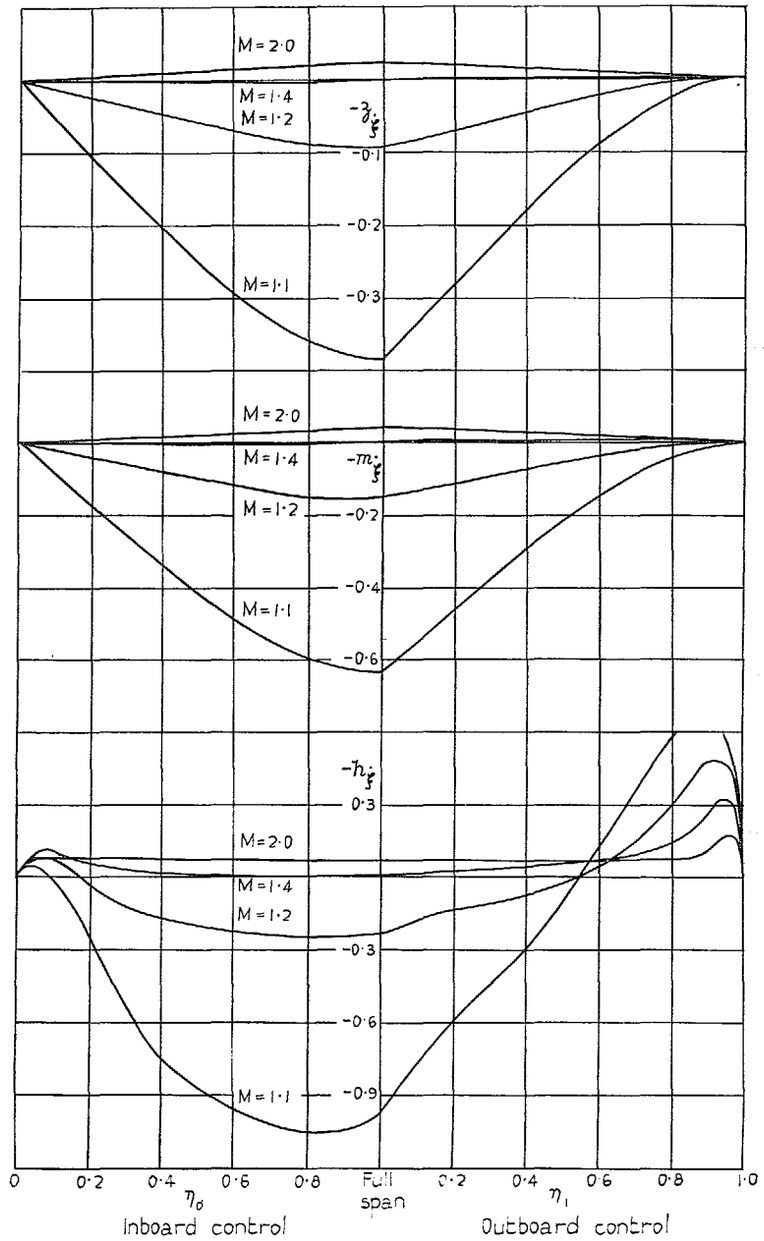

FIG. 14. Variation of damping derivatives with control span.

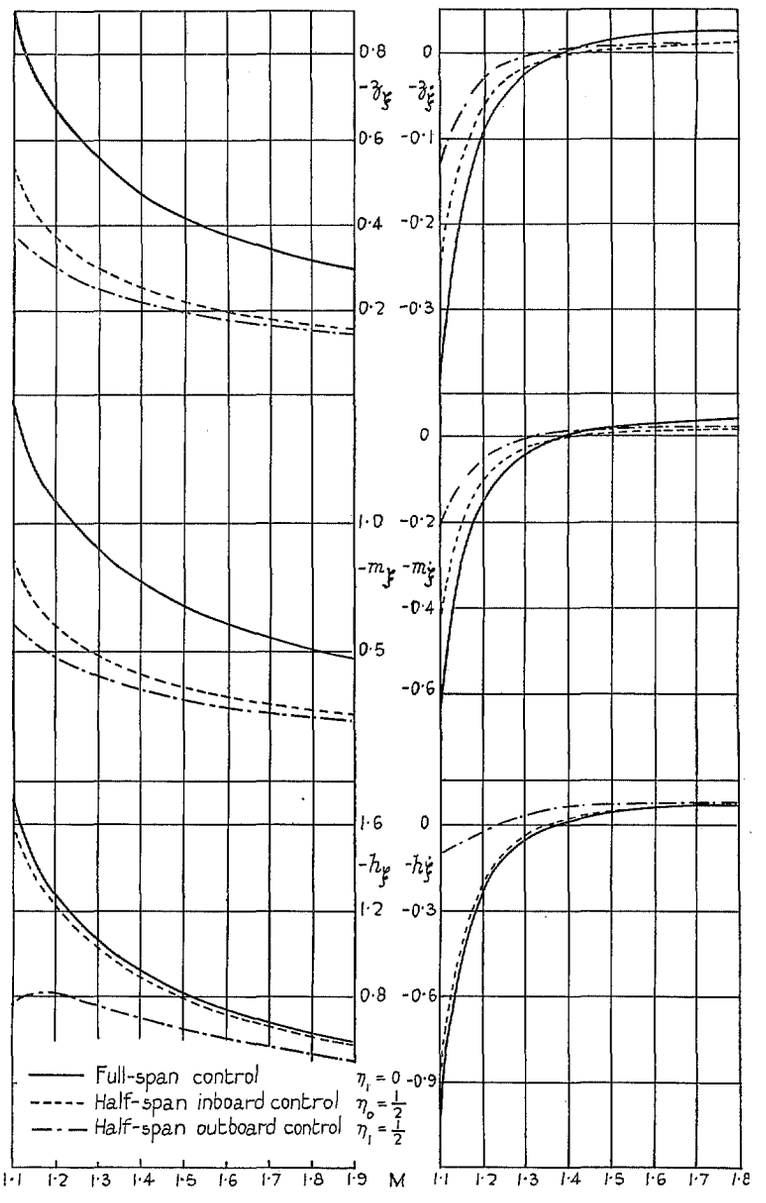

FIG. 15. Variation of control derivatives with Mach number.

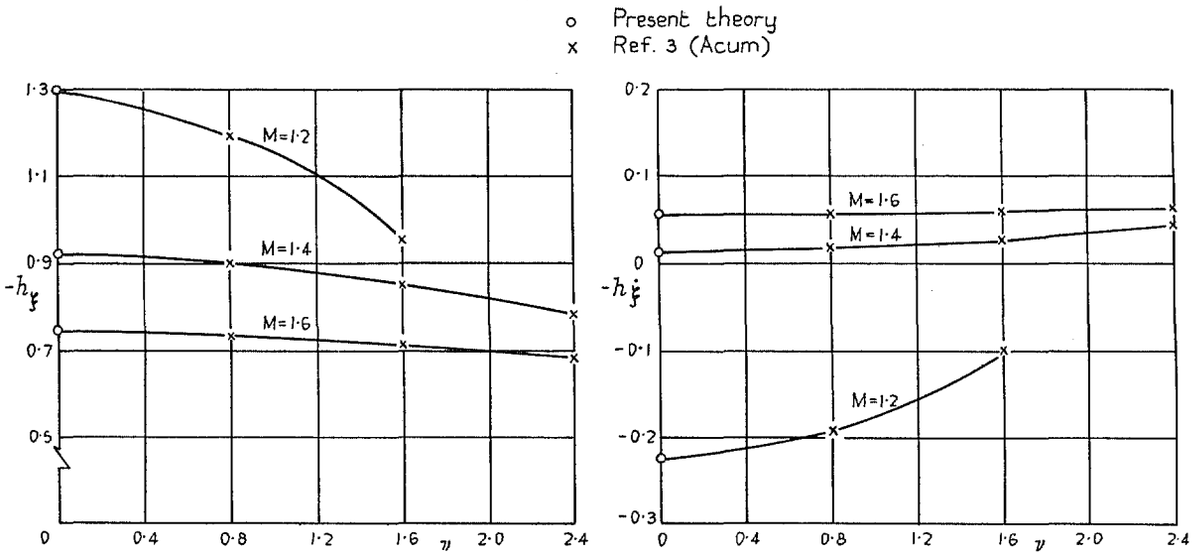

FIG. 16. Variation of full-span hinge-moment derivatives with frequency based on mean chord.

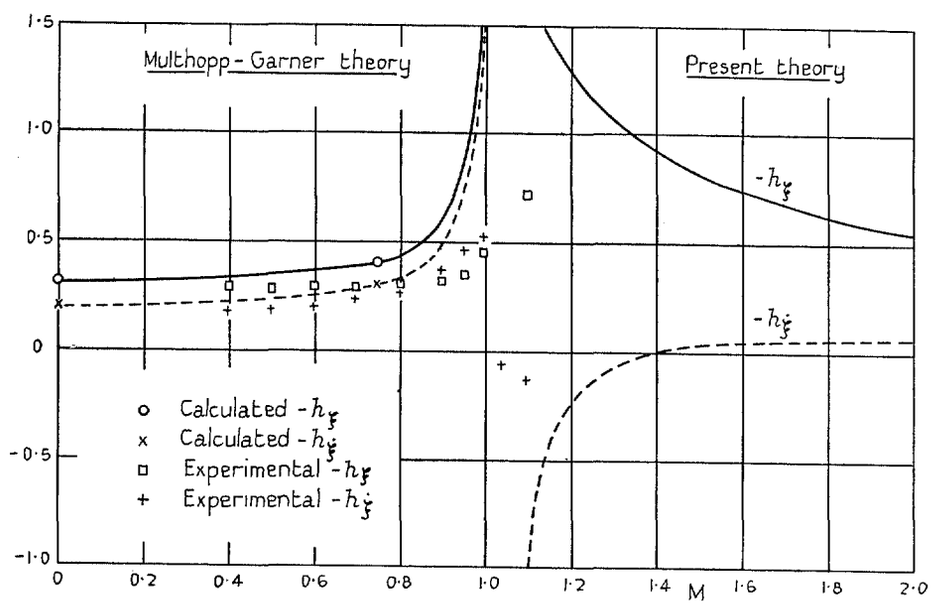

FIG. 17. Variation of full-span hinge-moment derivatives with Mach number.

(71241) Wt. 52/8943 K.7 2/58 Hw.

PRINTED IN GREAT BRITAIN

Publications of the Aeronautical Research Council

ANNUAL TECHNICAL REPORTS OF THE AERONAUTICAL RESEARCH COUNCIL (BOUND VOLUMES)

1939 Vol. I. Aerodynamics General, Performance, Airscrews, Engines. 50*s*. (52*s*.).
Vol. II. Stability and Control, Flutter and Vibration, Instruments, Structures, Seaplanes, etc. 63*s*. (65*s*.)

1940 Aero and Hydrodynamics, Aerofoils, Airscrews, Engines, Flutter, Icing, Stability and Control, Structures, and a miscellaneous section. 50*s*. (52*s*.)

1941 Aero and Hydrodynamics, Aerofoils, Airscrews, Engines, Flutter, Stability and Control, Structures. 63*s*. (65*s*.)

1942 Vol. I. Aero and Hydrodynamics, Aerofoils, Airscrews, Engines. 75*s*. (77*s*.)
Vol. II. Noise, Parachutes, Stability and Control, Structures, Vibration, Wind Tunnels. 47*s*. 6*d*. (49*s*. 6*d*.)

1943 Vol. I. Aerodynamics, Aerofoils, Airscrews. 80*s*. (82*s*.)
Vol. II. Engines, Flutter, Materials, Parachutes, Performance, Stability and Control, Structures. 90*s*. (92*s*. 9*d*.)

1944 Vol. I. Aero and Hydrodynamics, Aerofoils, Aircraft, Airscrews, Controls. 84*s*. (86*s*. 6*d*.)
Vol. II. Flutter and Vibration, Materials, Miscellaneous, Navigation, Parachutes, Performance, Plates and Panels, Stability, Structures, Test Equipment, Wind Tunnels. 84*s*. (86*s*. 6*d*.)

1945 Vol. I. Aero and Hydrodynamics, Aerofoils. 130*s*. (132*s*. 9*d*.)
Vol. II. Aircraft, Airscrews, Controls. 130*s*. (132*s*. 9*d*.)
Vol. III. Flutter and Vibration, Instruments, Miscellaneous, Parachutes, Plates and Panels, Propulsion. 130*s*. (132*s*. 6*d*.)
Vol. IV. Stability, Structures, Wind Tunnels, Wind Tunnel Technique. 130*s*. (132*s*. 6*d*.)

Annual Reports of the Aeronautical Research Council—

1937 2*s*. (2*s*. 2*d*.) 1938 1*s*. 6*d*. (1*s*. 8*d*.) 1939–48 3*s*. (3*s*. 5*d*.)

Index to all Reports and Memoranda published in the Annual Technical Reports, and separately—

April, 1950 - - - - R. & M. 2600 2*s*. 6*d*. (2*s*. 10*d*.)

Author Index to all Reports and Memoranda of the Aeronautical Research Council—

1909—January, 1954 R. & M. No. 2570 15*s*. (15*s*. 8*d*.)

Indexes to the Technical Reports of the Aeronautical Research Council—

December 1, 1936—June 30, 1939	R. & M. No. 1850	1*s*. 3*d*. (1*s*. 5*d*.)
July 1, 1939—June 30, 1945	R. & M. No. 1950	1*s*. (1*s*. 2*d*.)
July 1, 1945—June 30, 1946	R. & M. No. 2050	1*s*. (1*s*. 2*d*.)
July 1, 1946—December 31, 1946	R. & M. No. 2150	1*s*. 3*d*. (1*s*. 5*d*.)
January 1, 1947—June 30, 1947	R. & M. No. 2250	1*s*. 3*d*. (1*s*. 5*d*.)

Published Reports and Memoranda of the Aeronautical Research Council—

Between Nos. 2251–2349	R. & M. No. 2350	1*s*. 9*d*. (1*s*. 11*d*.)
Between Nos. 2351–2449	R. & M. No. 2450	2*s*. (2*s*. 2*d*.)
Between Nos. 2451–2549	R. & M. No. 2550	2*s*. 6*d*. (2*s*. 10*d*.)
Between Nos. 2551–2649	R. & M. No. 2650	2*s*. 6*d*. (2*s*. 10*d*.)
Between Nos. 2651–2749	R. & M. No. 2750	2*s*. 6*d*. (2*s*. 10*d*.)

Prices in brackets include postage

HER MAJESTY'S STATIONERY OFFICE

York House, Kingsway, London W.C.2; 423 Oxford Street, London W.1; 13a Castle Street, Edinburgh 2; 39 King Street, Manchester 2; 2 Edmund Street, Birmingham 3; 109 St. Mary Street, Cardiff; Tower Lane, Bristol 1; 80 Chichester Street, Belfast, *or through any bookseller.*

S.O. Code No. 23-3059